PHOTOELECTRIC EMISSION AND WORK FUNCTION OF SEMICONDUCTING DIAMONDS

By

WHUA FU WEI

Bachelor of Science
National Chekiang University
Hangchow, China
1943

Master of Science
Oklahoma State University
Stillwater, Oklahoma
1951

Submitted to the Faculty of the Graduate School of
the Oklahoma State University
in partial fulfillment of the requirements
for the degree of
DOCTOR OF PHILOSOPHY
August, 1965

PHOTOELECTRIC EMISSION AND WORK FUNCTION

OF SEMICONDUCTING DIAMONDS

Thesis Approved:

Thesis Adviser

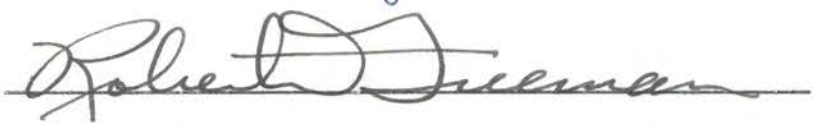

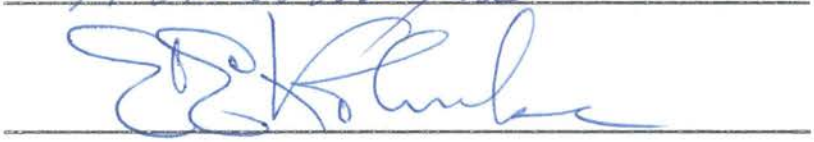

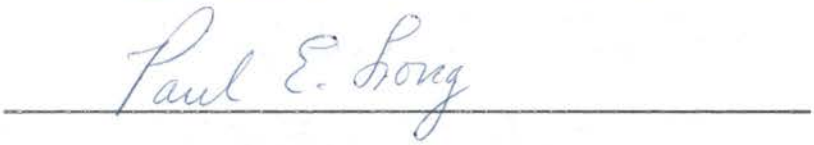

Dean of the Graduate School

ACKNOWLEDGMENTS

The author wishes to express his deepest gratitude to Dr. W. J. Leivo for the opportunity to do this research and for his valuable guidance in carrying out the experiment. The help and interest of Dr. J. F. H. Custers, Research Consultant, Industrial Distributors (1946) Limited and Dr. H. B. Dyer, Director of Research of the Diamond Research Laboratory, South Africa, in supplying the semiconducting diamonds are appreciated. He is indebted to Drs. F. C. Todd and M. D. Bell for their enlightening discussions and to Dr. H. E. Harrington for his helpful encouragement. Thanks are also due J. B. Krumme, K. J. Russell, C. J. Northrup and J. P. King for helpful comments and assistance, and Mr. M. W. Adkins for the construction of the glass apparatus.

Finally the author is grateful for the financial support for this research by the Electronic Systems Division, Air Force Systems Command, Laurence G. Hanscom Field, Bedford, Massachusetts.

TABLE OF CONTENTS

LIST OF TABLES

LIST OF FIGURES

CHAPTER I

INTRODUCTION

The Structure of Diamond Crystals

In the past fifteen years developments in the field of semiconductor physics and the applications of semiconducting materials have stimulated great interest in the diamond type crystals. In order to understand the properties of such valence crystals, the investigation of the electronic structure of diamond crystals appears to be fundamentally important. The diamond crystal is an assembly of carbon atoms held together by covalent bonds. Each bond joining two atoms consists of two electrons of opposite spins, each atom having the four nearest neighbors placed symmetrically around it at the vertices of a regular tetrahedron. The tetrahedrons are arranged so as to form a cubic diamond lattice. The diagram in Fig. 1 shows how the carbon atoms represented by balls are arranged and how each atom forms with its nearest neighbors four bonds represented by rods. The lattice constant, denoted by a, is the cube's edge in this figure and is 3.56 Å. The distance between the nearest neighbors is 1.54 Å. In comparison with other elemental semiconductors such as germanium, of which the lattice constant is 5.65 Å and the distance between the nearest neighbors is 2.44 Å, the carbon atoms in diamond are obviously more tightly bound than the germanium atoms in the germanium crystal. Spectrographic analysis has detected the presence of small amounts of impurities in all diamonds.

These include aluminum, copper, iron, calcium, magnesium, to mention just a few. Such impurity atoms may occupy the normal positions of the carbon atoms or occupy the interstitial sites. However, it is believed that impurity atoms of elements in the III-V groups enter the lattice by substitution for normal atoms, rather than by going into interstitial positions. Although the amount of such foreign elements is very small compared to the total number of atoms, their presence determines many of the important physical properties of the diamonds.

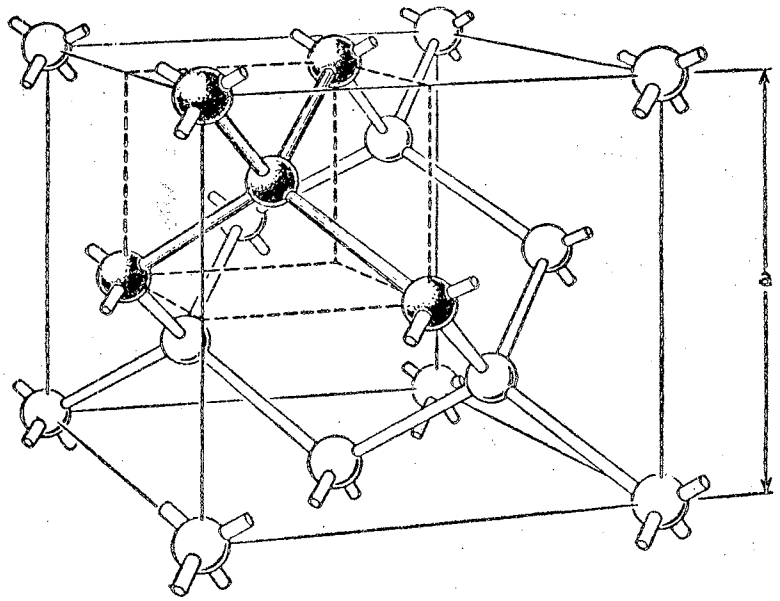

Fig. 1. Diamond structure, showing atomic arrangement and bond connections [after W. Shockley, (1)].

In the formation of solids atoms are closely packed together. Owing to the interatomic forces, the sharp discrete energy levels of the free atoms are broadened into bands of continuous levels which is the case in crystals. The broadening of the energy levels of the outermost valence electrons is particularly appreciable. In a perfect diamond crystal all the valence electrons are in the valence bands, leaving

the conduction bands empty. Herman (2), by using the orthogonalized plane wave method, has obtained much information about the energy bands in diamond. His results are presented in Fig. 2. Three valence bands, all of which have a single maximum at $\bar{k} = 0$, neglecting spin orbit interaction are degenerate at the reduced zone at their highest energy. Three conduction bands are also degenerate at the center of the zone, but the lowest energy for the conduction band occurs at six points along the six <100> directions in the zone. The indirect energy gap at 295° K obtained from the absorption data is 5.470 ± 0.005 eV. The corresponding value for the direct energy gap, obtained from the reflexion data is 7.02 ± 0.02 eV (3).

Robertson, Fox and Martin (4) made a systematic investigation in 1934 of the optical and electrical properties of two to three hundred diamonds. From the results of the optical transmission and photoconductivity studies, they classified diamonds into Type I diamonds and Type II diamonds. Type I diamonds have an absorption band at 8 μ in the infrared region and are opaque, or nearly so, to the ultraviolet light beyond 3000 Å, while the Type II diamonds have no absorption band at 8 μ and are transparent to 2250 Å. Photoconductivity measurements showed much larger photocurrents produced by Type II than by Type I diamonds. There are other differences between these two types of diamonds such as fluorescence, x-ray diffraction patterns, birefringence and so forth.

In 1952 J. F. H. Custers (5) discovered a diamond having the properties of Type II diamond, but it had a pronounced electrical conductivity and showed phosphorescence after exposure to short wavelengths of ultraviolet light. He designated it Type IIb diamond, while

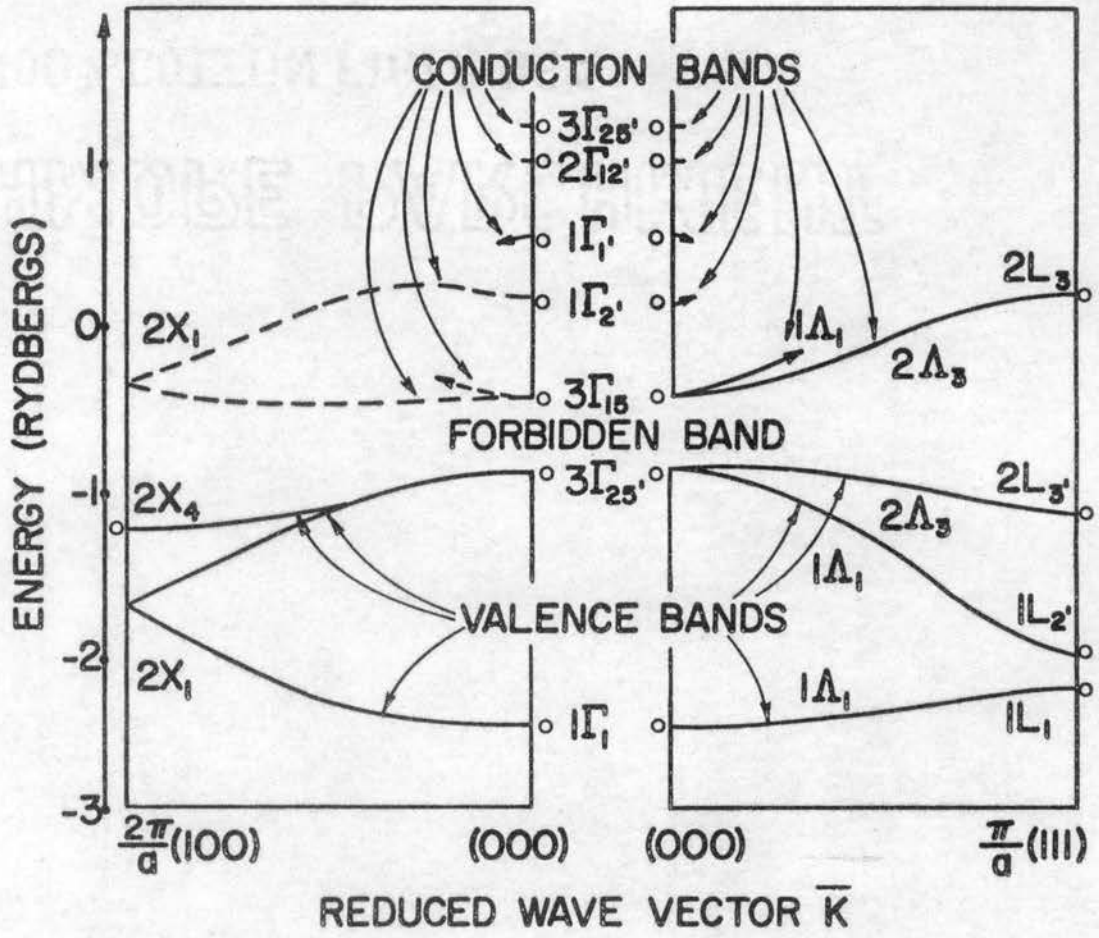

Fig. 2. Energy band structure of diamond. The curves have horizontal slopes at points marked o. (After F. Herman (2)).

the other Type II diamonds were referred to as Type IIa. Such natural conducting diamonds are rare. Twenty-one were known to exist in 1954 (6).

Electron Emission from Diamonds

Electrons may be removed from a solid in a number of ways. Thermionic emission refers to removal by heat, photoelectric emission to removal by a photon, and field emission to removal by quantum mechanical tunnelling in an electric field. Electrons can also be dislodged from an atom upon colliding with other energetic electrons or ions; such electrons are called secondary electrons. Because of important applications, electron emission from most metals has been extensively studied in one way or another. Electron emission from diamond, however, has not been successfully observed. This is presumably due to the following reasons: the graphitization of diamonds at high temperatures, the tight binding of carbon atoms, and the high resistivity of the regular insulating diamonds. Such properties make the measurements difficult to carry out.

Tartakowsky (7) tried to determine the work function of diamond along with other insulating substances -- mica, sulphur, rock salt and paraffin -- by the external photoelectric effect. He suggested that the work function of a crystal may be divided into two parts: W_1, the work necessary to set the electron free within a crystal and bring it to the surface; and W_2, the work necessary to take it from the surface. In his view, the energy of a photon which produces a photoelectron from the charged surface corresponds to the work W_2. The only sample he had was a somewhat colored insulating diamond. In his experiment, the sample

was mounted inside an evacuated photocell. The diamond surface was first bombarded by slow electrons so that a surface charge was formed as it had been in the case of other kinds of insulating samples which he had investigated earlier. The surface was then exposed to the ultraviolet light of a mercury lamp through a quartz window immediately after the bombardment of the electrons, and the photoelectric emission current was measured with a quadrant electrometer. His experiment showed that no appreciable surface charge was formed by the bombardment and he stated that the electrons appeared to be penetrating into the diamond instead of being liberated from it during the irradiation. He concluded that there was no photoelectric emission from the diamond. So far this is the only experimental investigation on the photoelectric emission of electrons from diamond which we have found in literature. It should be noted that the shortest wavelength of a strong line which the mercury lamp is able to give is 2537 Å. This is longer than the shortest wavelength of the intrinsic activation of the diamond which is 2250 Å (4). Light of shorter wavelengths from the mercury lamp is extremely weak. Thus, very few electrons could be expected to be emitted from the diamond. On the other hand, more electrons could be produced from other materials within the photocell by the reflecting light and could contribute to the feeble current being observed. This current flowing in a reverse direction corresponds to the electrons penetrating into the crystal.

Present Investigations

The main purpose of the present investigation is to detect the phenomenon of photoelectric emission and to determine the position of

the Fermi level in the energy spectrum for electrons of semiconducting diamonds. If the position of the Fermi level with respect to the vacuum is known, the photoelectric work function is determined. The work function is defined as the energy required to remove an electron from inside the surface of a crystal, at the Fermi level, to rest at a point just outside the surface of the crystal. The distance from this point to the surface is large enough so that the image potential is negligible but is small compared with macroscopic dimensions. Thus the results of these measurements can give information relating to these states normally occupied and produce a picture of the energy structure of the diamond at the surface of the crystal. Such information is valuable in understanding the diamond crystal and may be important in practical applications in the near future.

In view of the large energy gap of the diamond crystal as well as the tightly bound carbon atoms in the diamond, a plan was set up for the investigation of photoelectric emission phenomenon of semiconducting diamonds by extreme ultraviolet light. A carbon arc, which has rich intense lines in this region, was employed as a light source (8). The arc was operated either in a dry nitrogen atmosphere or in the air. Lithium fluoride windows were used for the photoelectric cells. Both dry nitrogen and lithium fluoride are transparent to light of wavelengths longer than 1050 Å (9, 10).

CHAPTER II

THEORIES OF PHOTOELECTRIC EMISSION AND WORK FUNCTION

Koopmans' Theorem on the Work Function of a Solid

The work function of a solid is closely related to the cohesive energy. The work function is high if the cohesive energy is high. Its value is affected by the surface conditions involving the orientation, oxide layer and deposition of impurities. Therefore, the work function is determined by the binding properties as well as the surface structure.

Let us consider a solid bounded by a plane. The atoms in the interior of the solid are equally acted upon by the interatomic forces and are uniformly distributed. On the other hand, the ones on the surface are distributed differently because the interatomic forces change rapidly at the boundary. These interatomic forces are almost entirely electrostatic in nature, but there are kinetic effects arising from the motion of the electrons. As to the external effects on the surface, the net results are to produce a dipole moment which may be positive or negative.

According to Koopmans' theorem (11) the energy required to remove a single electron in the state ψ_k from the crystal is equal to the negative parameter $E(\bar{k})$ in Fock's equation, namely,

$$-\frac{\hbar^2}{2m}\Delta\psi_k(\bar{r}_1) + [V(\bar{r}_1) + e^2\int\frac{\rho(\bar{r}_2)}{r_{12}}d\tau_2 + A(\bar{r}_1)]\psi_k(\bar{r}_1) = E(\bar{k})\psi_k(\bar{r}_1), \quad (2.1)$$

$V(\bar{r}_1)$ is the total ion-core potential, $\rho(r_2)$ is the valence electron distribution and

$$V(\bar{r}_1) + e^2\int\frac{\rho(\bar{r}_2)}{r_{12}}\,d\tau_2 \tag{2.2}$$

is the Hartree potential of the crystal at a point inside the lattice, it differs from the potential for a crystal in which the dipole is zero by the term $4\pi eP_n$. The operator $A(\bar{r}_1)$ comes from the exchange correlation hole. The ψ_k has the form $X_k(\bar{r})e^{i2\pi\bar{k}\cdot\bar{r}}$ in the Bloch scheme and $X_k(\bar{r})$ has the translational periodicity of the lattice. φ_i is the product of ψ_i and a spin function.

Multiplying Fock's equation by ψ_k^* and integrating, we obtain

$$E(\bar{k}) = -\frac{\hbar^2}{2m}\int\psi_k^*\Delta\psi_k d\tau_1 + \int|\psi_k|^2[V'(\bar{r}_1) + e^2\int\frac{\rho(\bar{r}_2)}{r_{12}}d\tau_2]d\tau_1$$

$$+ \int\psi_k^* A\psi_k d\tau_1 + 4\pi eP_n. \tag{2.3}$$

Here,

$$V'(\bar{r}_1) + \int\frac{e^2\rho(\bar{r}_2)}{r_{12}}d\tau_2 \tag{2.4}$$

is the Hartree potential for a lattice having no surface dipole.

The correlation energy of the uppermost electron in the filled band has been calculated by Wigner (12), and the exchange energy has been evaluated by Seitz (11). The latter has shown that the energy E_W required to remove an uppermost electron is given by the equation

$$-E_W = E_o + \frac{5}{3}E_F + 1.2\frac{e^2}{r_s} - 0.612\frac{e^2}{r_s} + g(r_s) - r_s\frac{g'(r_s)}{3} + 4\pi eP_n, \tag{2.5}$$

where r_s is the radius of the sphere which replaces the cellular polyhedron chosen for a unit cell in the sphere approximation, E_F is the Fermi energy, $1.2\ e^2/r_s$ is the Coulomb energy, $0.612\ e^2/r_s$ is the exchange energy and $g(r_s) - r_s\ g'(r_s)/3$ is the correlation energy for the uppermost electron in the filled band. E_o is the energy parameter in the wave equation including a radial potential field.

In terms of cohesive energy per atom ϵ_c, and ionization potential of the free atom I(Z), equation (2.5) becomes

$$E_W = 1/Z\ [\epsilon_c + I(Z)] + [-\frac{2}{3}E_F - 0.6\frac{e^2}{r_s} + \frac{0.458\ e^2}{3r_s} + \frac{r_s g'(r_s)}{3} - 4\pi eP_n, \quad (2.6)$$

where Z is the number of valence electrons per atom.

The quantities in equation (2.6) except P_n have been computed for a few metals with one valence electron. Close agreement between the observed values of E_W and the computed values of $E_W + 4\pi eP_n$ for these metals shows that the surface dipole moment is very small for clean metal surfaces. Calculations for solids with more than one valence electron per atom would be very complicated. However, equation (2.6) is the result of a fundamental treatment, and it shows the significant quantities contributing to the work function of a solid.

Statistical Evaluation of Work Function

The work function of a metal has been treated by Fowler (13) on the basis of Sommerfeld's free electron theory of a metal. In his evaluations the electron gas is considered to be obeying strictly the Fermi-Dirac statistics. The probability of a state of energy E, occupied by an electron is given by

$$f(E) = \frac{1}{1 + \exp[(E - E_F)/kT]}. \qquad (2.7)$$

where E_F is the Fermi energy, k the Boltzmann constant and T the absolute temperature.

The value of the Fermi energy is a function of electron concentration n, and temperature. At absolute zero, all states up to the Fermi level $E_F(0)$ are occupied, all higher states are empty of electrons. Quantum theory treatment for free particles in a box shows the Fermi energy at absolute zero as (14)

$$E_F(0) = \frac{h^2}{2m}\left(\frac{3n}{8\pi}\right)^{2/3} \qquad (2.8)$$

The Fermi energy at absolute zero is a function of electron concentration only. The order of magnitude of $E_F(0)$ measured from the bottom of the conduction band is about 5 eV.

At a temperature above absolute zero, the change in the distribution function from its form at absolute zero takes place when close to $E_F(0)$. By series expansion for E_F, Kittel (14) shows that the Fermi energy is decreasing. The result is given by

$$E_F \cong E_F(0) - \frac{\pi^2}{12}\frac{k^2T^2}{E_F(0)} \qquad (2.9)$$

The change in Fermi energy is, however, very small at attainable temperature and may be neglected.

By applying thermodynamic formulas to the electron gas, Fowler (13) obtains the free energy, the total energy, the absolute activity and the partial potential of the electron gas. The internal structure of the metal is neglected so that the electrons are assumed to move in a region of uniform potential energy $-E_o$, their potential energy in free

space just outside the metal being taken as zero. From such quantities he computes E_W, the average energy required to take a single electron at constant temperature T and volume V from the interior of the metal to rest outside the metal leaving behind an equilibrium distribution; the result is

$$E_W = E_o - \frac{3}{5} E_F(0) + \frac{\pi^2}{12} \frac{k^2T^2}{E_F(0)} \tag{2.10}$$

Let η_o, be the work needed to take a single valence electron from the lowest state inside the metal to a state of rest outside the metal. This work is not equal to E_o, because the removal of a single electron changes N/V, the ratio of the total electrons to the volume of the metal, and so the value of η_o for the remaining electrons. This process does not leave behind an equilibrium distribution, since it leaves the lowest state empty. The value of η_o is given by

$$\eta_o = E_W + E_F(0) + \frac{\pi^2}{12} \frac{k^2T^2}{E_F(0)} \tag{2.11}$$

This is the same result obtained by Kittel in regard to Fermi energy. As mentioned earlier, the term in T^2 is negligible in almost all applications, and equation (2.11) reduces to

$$\eta_o = E_W + E_F. \tag{2.12}$$

We are interested in the action of light for the removal of electrons from a solid. When light falls on a cold solid surface, electrons are emitted as soon as the frequency ν of the exciting light exceeds a certain threshold frequency ν_o. At such a frequency, the photon transfers all its energy to the electron which it emits. This is known as the photoelectric effect. When $T \to 0$, there are no electrons in a conducting

solid with a kinetic energy greater than E_F, and many with any energy less than E_F. In order that an electron whose initial energy is E may emerge after absorbing a quantum of energy $h\upsilon$, it is necessary that

$$h\upsilon + E > \eta_o. \tag{2.13}$$

The least possible value which satisfies this equation is

$$h\upsilon = h\upsilon_o = \eta_o - E_F = E_W. \tag{2.14}$$

The photoelectric threshold frequency υ_o is thus equal to E_W/h. The theory demands a fairly definite average negative potential energy η_o for an electron inside a metal as compared with the outside, for we have $\eta_o = E_W + E_F$.

The foregoing treatment is based on Sommerfeld's free electron theory in metal; any periodic structure inside the metal is entirely ignored, except the potential barrier at the surface. When the periodic variations of potential inside the crystal are taken into account, the quantum theory of electrons provides a basis for the classification of the solids into metals, insulators and semiconductors.

In a metal, the photoelectrons, emitted by the action of the photon at an energy near the threshold, are originating at the conduction band close to the Fermi level. Therefore, the photoelectric threshold energy of the photon is equal to the work function. In a semiconductor, the photons interact with bound electrons, the photoelectrons originate at the valence band or at the impurity states which may or may not be in the neighborhood of the Fermi level. In general the photoelectric threshold energy is not equal to the work function.

We next consider the photoelectric emission and photoelectric threshold of a semiconductor.

Photoelectric Emission from Semiconductors

Fermi Level and Hole Concentration of a P-Type Semiconductor.

The position of the Fermi level for an extrinsic semiconductor at a constant temperature depends upon the concentration of electrons and holes. The hole concentration p in the valence band may be expressed as below for a single band (15),

$$p = 2\left(\frac{2\pi m^* kT}{h^2}\right)^{3/2} \exp[-(E_F - E_V)/kT], \qquad (2.15)$$

where m^* is the effective mass of hole, E_V is the top of the valence band.

Let N_a = density of acceptor ions

N_d = density of donor ions

p = concentration of holes

n = concentration of electrons

p_a = concentration of holes trapped in acceptor levels

n_d = concentration of electrons trapped in donor levels

The condition of electrical neutrality requires

$$n + n_d + N_a = p + p_a + N_d. \qquad (2.16)$$

In the case of a p-type semiconductor, where n and n_d are negligible compared with the concentration of free holes, equation (2.16) reduces to

$$p_a = N_a - N_d - p. \qquad (2.17)$$

The concentration of holes in the acceptor levels is given by the product of the density of acceptor levels and the probability that they

are occupied by a hole, or

$$p_a = N_a \cdot f_a \tag{2.18}$$

In accordance with Blakemore (15), an expression for the probability of an impurity acceptor level being occupied by a hole (or unoccupied by an electron) should include the impurity level spin degeneracy and the degeneracy of the valence bands. The spin degeneracy for a monovalent acceptor is two and the three valence bands of diamond are degenerate at $\bar{k} = 0$ neglecting spin orbit interaction. Therefore, the Fermi-Dirac factor applied to the p-type impurity states in a diamond becomes

$$f_a = \frac{1}{1 + 1/6 \exp[(E_F - E_a)/kT]}. \tag{2.19}$$

where E_a is the acceptor level. From the above three equations, we obtain an expression for the Fermi energy

$$E_F = E_a + kT \ln 6 \frac{N_d + p}{N_a - N_d - p}. \tag{2.20}$$

If the Fermi energy in equation (2.16) is replaced by the above expression, we obtain

$$p = \frac{N_a - N_d - p}{3(N_d + p)} \left(\frac{2\pi m^* kT}{h^2}\right)^{3/2} \exp[-(E_a - E_V)/kT]. \tag{2.21}$$

The quantity $(E_a - E_V)$ is the activation energy of the acceptors and is denoted by ϵ. Therefore

$$p = \frac{N_a - N_d - p}{3(N_d + p)} \frac{2\pi m^* kT}{h^2}^{3/2} \exp(-\epsilon/kT). \tag{2.22}$$

For a p-type diamond the activation energy of impurities is large, the value of p is much smaller than N_a and N_d at room temperature, therefore, the above equation may be written as

$$p = \frac{N_a - N_d}{3N_d} \left(\frac{2\pi m^* kT}{h^2} \right)^{3/2} \exp(-\epsilon/kT). \qquad (2.23)$$

By using equations (2.22) and (2.20), the concentration of holes and the Fermi energy may be calculated.

Photoelectric Threshold of Emission in a Semiconductor

Let us consider the case of an intrinsic semiconductor in which the photoelectrons originate at the valence band edge. The photoelectric threshold energy $h\nu_o$, in this case, is equal to the sum of the band gap E_G, and the electric affinity E_A, i.e.

$$h\nu_o = E_G + E_A. \qquad (2.24)$$

This is the energy relation for the intrinsic photoelectric emission. Such a relation is clearly shown in Fig. 3 (a), where E_c represents the bottom of the conduction band, and E_V the top of the valence band. From equation (2.24), E_A may be expressed in terms of $h\nu_o$, and E_G. The relationship between the photoelectric threshold of emission Φ and the work function E_W is given by

$$h\nu_o = E_W + \delta = \Phi \qquad (2.25)$$

where δ is the energy difference between the Fermi level and the top of the valence band.

If the concentration of the defect levels is high, electron densities at the defect levels are large enough to produce appreciable photoelectric emission, the threshold response is then determined by the energy difference between the vacuum level and the states which have large electron densities. In the case of an n-type semiconductor with a Fermi level halfway between the defect levels and the conduction band,

we have

$$h\nu_o = E_W + E_G - \delta. \qquad (2.26)$$

This relation is shown in Fig. 3 (b). Photoelectric threshold for a p-type semiconductor is shown in Fig. 3 (c).

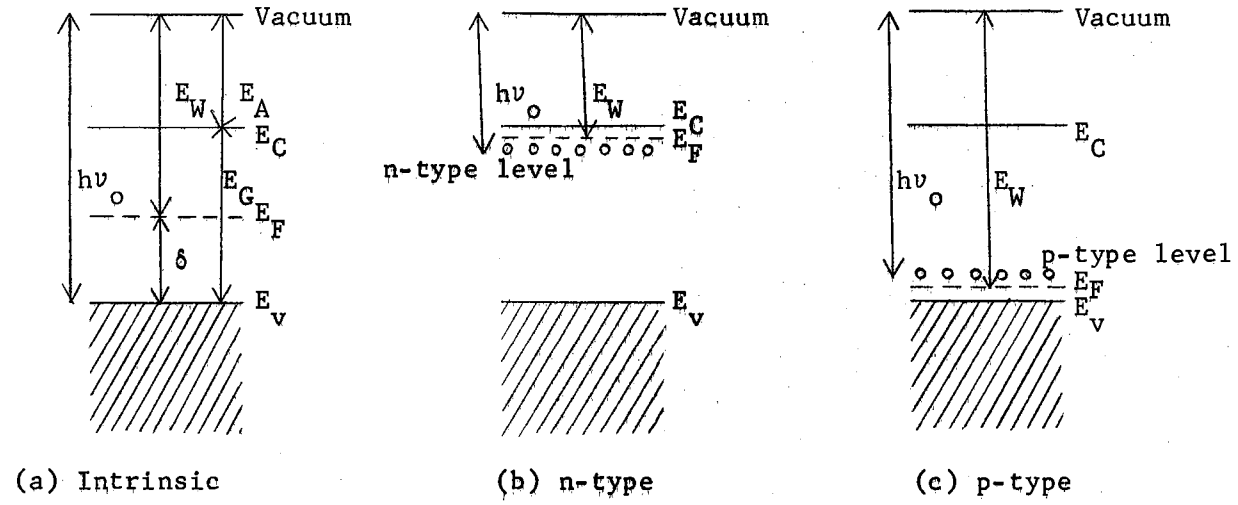

Fig. 3. Energy level diagram of semiconductor

By the action of the photons with threshold energy, some electrons which acquire sufficient energies will be excited into the states above the vacuum level, others, due to energy loss processes, notably the production of hole-electron pairs and lattice scattering, will arrive at the surface of the crystal with less than escape velocities.

Probability of Photoelectric Emission

Not all electrons which acquire energies greater than the threshold can escape from the surface of a solid. Van der Ziel (16) has derived the escape probability from a metal for an electron of energy E moving at an angle θ from the normal toward the surface. The condition for escaping is $\cos\theta = (W/E)^{1/2}$ for $E \geq W$. By setting $\cos\theta_o = (W/E)^{1/2}$, he obtained the probability of escaping

$$P(E) = 1 - \cos \theta_o = 1 - (W/E)^{1/2} \qquad (2.27)$$

where W is the energy difference between the bottom of the conduction band and the valence band. According to Van der Ziel, this equation applies also to semiconductors and insulators. Assuming this is true, the escape probability of an electron from a semiconductor will be larger than that from a metal generally. For in such cases, $W = E_A$, and $E = E_A + E_G$; the larger the E_G, the higher the P(E). The emission of electrons from diamond is most favorable because of its large energy gap.

Effects of Surface States on Photoelectric Emission

Shockley (17) has proved that surface states would be present on the surface of germanium and crystals having the diamond lattice. The states may be considered as the unfilled orbitals or dangling bonds of the surface atoms, with the maximum density corresponding to that of the surface atoms. According to Pugh (18), there are no surface states for the diamond near the center of the forbidden zone, but there is a band of surface states in the lower part of the forbidden zone. Taking account of the surface states, the energy bands of a semiconductor are bent at the surface.

An oxide layer and adsorbed impurities are normally present on the surface of a semiconductor (19). This layer contains positive or negative charges in the surface states. The charges in the outer surface are referred to as slow surface charges and those in the inner surface are referred to as fast surface charges. If we let Σ_{ss} be the density of charges trapped in the slow surface states, and Σ_{sf} that in the fast surface states, the following relation holds.

$$\Sigma_{ss} + \Sigma_{sf} + \Sigma_{sc} = 0 \qquad (2.28)$$

Σ_{sc} is the density of charges in the space charge layer. The external conditions determine the density of the slow surface charges; it is counterbalanced by the sum of charges in the fast states and in the space charge layer. The space charges extend in depth into the semiconductor and form the potential barrier. Electrons and holes from the space charge region are often trapped in the energy states in the forbidden zone to attain equilibrium. Such energy states are fast surface states and are identified with the Tamm surface states (20).

If the total charge in slow and fast states is positive ($\Sigma_{ss} + \Sigma_{sf} > 0$), the surface potential is higher than the bulk potential and the energy bands bend downward from the bulk toward the surface, Therefore, in an n-type semiconductor, the electron concentration will increase toward the surface. The result is an n-type surface on an n-type semiconductor as shown in Fig. 4(a). In a p-type semiconductor, a corresponding layer exhausted of holes is formed on the surface. This exhaustion of holes can make the concentration of electrons exceed the concentration of holes in this layer. This results in an n-type surface on a p-type semiconductor and in a large band bending as shown in Fig. 4(b).

When the total charge in the slow and fast surface states is negative ($\Sigma_{ss} + \Sigma_{sf} < 0$), the surface potential is lower than the bulk potential and the energy bands bend upward from the bulk toward the surface. Therefore, in an n-type semiconductor, electrons are moving away from the surface. The exhaustion of electrons can make the concentration of holes higher than that of electrons. Thus it results in a p-type surface on an n-type semiconductor as shown in Fig. 4(c). While

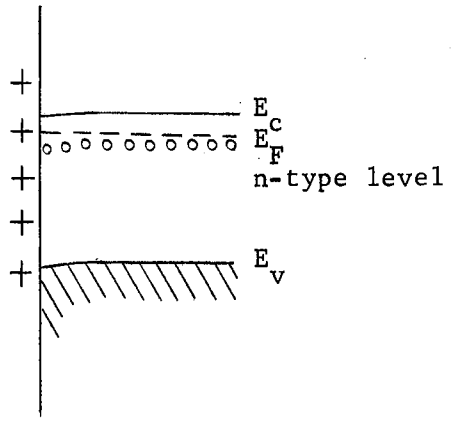

(a) N-type semiconductor with positive surface charges

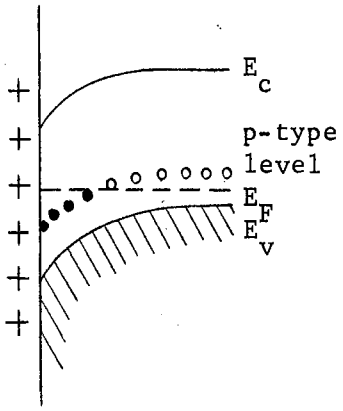

(b) P-type semiconductor with positive surface charges

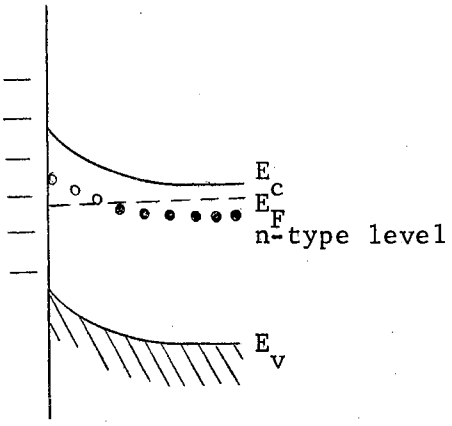

(c) N-type semiconductor with negative surface charges

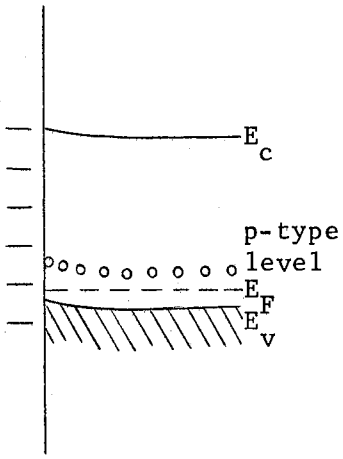

(d) P-type semiconductor with negative surface charges

Fig. 4. Potential barrier at the surface of n-type and p-type semiconductors with different sign of surface charge

in a p-type semiconductor holes flow toward the surface, and the concentration of holes is thus increased at the surface. The result is a p-type surface on a p-type semiconductor, as shown in Fig. 4(d).

The energy band bending in the space charge region has a direct effect on the energy difference between the vacuum level and the band edge at the surface since the space charge band bending builds up an electric field around the surface. If the band bending is downward, the electric field is into the surface, and any electron excited in the interior of the semiconductor will be accelerated toward the surface. Thus, the downward band bending will aid the photoelectric emission and will reduce the photoelectric threshold energy. On the other hand, an upward band bending will retard the electrons moving to the surface and will increase the photoelectric threshold energy. The depth of origin of the photoelectrons depends upon the absorption coefficient of the material for the radiation. If the maximum depth of origin of the photoelectrons is comparable to or greater than the space-charge depth, an appreciable fraction of the emission will be characteristic of a raised or lowered threshold.

Photoelectric emission from defect energy states in the forbidden zone were observed in semiconducting materials of both n-type and p-type. Spicer (21), in investigating the photoelectric emission of n-type CsAu, found that the photoelectrons were excited from the defect levels near the bottom of the conduction band. Spicer (21) also investigated the photoelectric emission of alkali antimonides at 300° K and 77° K; these results were compared. The spectral yields were found to be lower, and the threshold energy was found shifted higher in the case of the lower temperature. The changes were due to the freeze-out of

the impurities. Therefore, he confirmed that the photoelectrons from the p-type semiconductor at the low yield area originated at the filled acceptor energy states. Scheer and Van Laar (22) also observed photoelectrons originating at filled surface states in p-type silicon.

Photoelectric emission from KI and RbI containing F-centers observed by Apker and Taft (23) was exciton-enhanced. When a photon energy greater than the energy gap E_G is absorbed in a crystal, electrons and holes are produced. The electrons and holes are free to move independently through the crystal giving rise to conductivity. But they may form a stable exciton. In the case of KI or RbI, excitons were formed by the action of the photons. Some of the excitons gave up their energies to F-centers ejecting the F-center electrons from the crystal, and a lower, broad threshold energy was observed.

When the photon energy is near the threshold value for production of photoelectrons, the photoelectric emission is assumed to take place only at the surface of the crystal. When the photon energy is higher than the threshold value, the photoelectric emission from the bulk of the crystal will dominate. The photoelectric theory of metals by Tamm and Schubin (24) shows that an appreciable number of electrons are ejected at some depth within the metals only when the photon energies are in the order of twice the threshold value. Taft and Apker (25) observed no electron-electron scattering and no drastic changes in the photoelectron energy distributions at a photon energy not more than twice the threshold for Cs_3Sb and Rb_2Te.

Fowler's Theory on Photoelectric Yield of Metals

Fowler (26) has derived a simple theory giving the photoelectric yield for clean metal as a function of the photon energy near the

threshold. In doing this he first evaluated, based upon Sommerfeld's free electron theory, the density of available electrons for ejection having velocity component normal to the surface. By assuming equal probability of excitation and escape he derived an expression between the photocurrent I and the photon energy $h\nu$

$$\log I/T^2 = B + f\left(\frac{h\nu - h\nu_o}{kT}\right), \qquad (2.29)$$

where B is a constant independent of temperature T and frequency ν, k is the Boltzmann constant and $h\nu_o$ is the threshold energy for production of photoelectrons. The threshold curve $f[(h\nu - h\nu_o)/kT]$ may be plotted as a function of $(h\nu - h\nu_o)/kT$. Now, supposing the observed values of the photoelectric current are plotted in the form of $\log I/T^2$ as a function of $h\nu/kT$, it is seen that, if the observed curve is shifted horizontally by an amount $h\nu_o/kT$ and vertically by an amount B, it should coincide with the theoretical curve. The horizontal shift determines the threshold ν_o. This theory has been proved useful and very successful for many metals.

Theories of Photoelectric Emission from Semiconductors

The electron distribution in a metal is different from that in a semiconductor. For example, the concentration of the electrons in the conduction band is negligible in a pure semiconductor if the forbidden gap is larger than half of 1 eV; therefore, the photoelectric theories for metals are not applicable to semiconductors. Although precise theory concerning the photoelectric emission from semiconductors has been lacking, a few prominent works are presented here briefly.

Huntington and Taft (27) have evaluated the transition probability for the photoemission of an electron with initial energy E near the top of the valence band E_v in a semiconductor. They considered the value of

$h\nu$ appreciably larger than the photoelectric threshold $h\nu_o$ required for an electron emission from the state E_v. The density of states goes to zero as $(E_v - E)^{1/2}$ and the value of emergent fraction is a slowly varying function of E near E_v, going to zero like $(E_v - E) \simeq h(\nu - \nu_o)$. These factors dominate the photoelectrons from initial states near E_v. Therefore, the energy distribution of the emitted electrons, expressed as the product of the two factors, goes to zero like $(E_v - E)^{3/2}$ and the photoemission current is a function of $(h\nu - h\nu_o)^{3/2}$. Data obtained on Te, Ga, As, Sb and Bi were in agreement with this result but that obtained on Ge showed the photoemission as a function of $(h\nu - h\nu_o)^2$, (28). Redfield (29) has extended further this calculation.

Spicer (21), in studying photoelectric emission from semiconducting alkali-antimonide compounds, proposed: (1) the conduction and valence bands are parabolic with extrema at the same $\bar{k}$ value; (2) absorption is divided into two types, $\alpha_c(h\nu)$ representing the absorption coefficient for all the transitions in which the final state lies below the vacuum level, and $\alpha_p(h\nu)$ representing the transitions to levels above the vacuum level. The total absorption coefficient $\alpha_t(h\nu)$ is equal to the sum of α_p and α_c; (3) P(x, $h\nu$), the probability of escape is equal to $B(h\nu)e^{-\beta x}$, where $B(h\nu)$ is an undefined function of $h\nu$ and B is a constant. Under these assumptions he obtained a general form for the yield

$$Y(h\nu) = \frac{\alpha_p(h\nu)}{\alpha_t(h\nu) + \beta} B\ (h\nu). \qquad (2.30)$$

In applying this result to alkali-antimonide compounds, he obtained

$$Y\ (h\nu) = \frac{[h\nu - (E_G + E_A)]^{3/2}}{[h\nu - (E_G + E_A)]^{3/2} + Q} B\ (h\nu), \qquad (2.31)$$

where $Q = (\alpha_c + \beta)/C$ is a parameter determined by the fitting of experimental data, C is a constant and α_c is nearly constant for these compounds. The theoretical curve fitted well to some of his experimental data while deviating from the results of some other data.

A systematical study for all possible cases of the photoelectric emission from semiconductors was made by Kane (30). The relation between yield and photon energy was determined for a number of possible photoelectric productions and for various escape mechanisms involving volume and surface states in semiconductors. Two major excitation processes are involved in both the volume production and the surface band states production of the photoelectrons. They are direct optical transition, in which the initial and final states differ in $\bar{k}$ vector only by the photon $\bar{k}$ vector, and indirect optical transition or phonon assisted transition. In the case of volume production, the yield from direct transition is proportional to $(h\upsilon - h\upsilon_o)$ and that from indirect transition is proportional to $(h\upsilon - h\upsilon_o)^{5/2}$. In the production of surface band states for the threshold greater than E_F, the yields are $(h\upsilon - h\upsilon_o)$ and $(h\upsilon - h\upsilon_o)^2$ respectively for direct and indirect transitions. The result of his evaluation for the emission from the surface imperfection states below the Fermi level consists of the term $(h\upsilon - h\upsilon_o)$. These results are useful in inferring the product mechanism from the yield curve.

In investigating the photoelectric emission from silicon, Gobeli and Allen (31) developed a theoretical model for interpreting their experimental data. Since the band structure of diamond is similar to that of silicon, we are particularly interested in it. The general principal is presented here.

We first discuss the emission from an intrinsic semiconductor which has a constant valence band to the surface. Two excitation processes at the surface are considered, one arising from indirect optical absorption and the other from direct absorption. This is illustrated in Fig. 5(a). The maximum of the valence band V is assumed to be lying at $\overline{k}$ (000) as is the minimum of the conduction band C. By taking the top of the valence band as the zero of the energy, the minimum separation of the bands is a direct energy gap of magnitude E_d, which is shown less than the height of the vacuum level.

The photoelectrons must be excited into a final state of band C which lies above the vacuum level. For the indirect transition, in which phonon interactions conserve momentum, transitions between arbitrary states of the V band and C band are possible provided only that they are energetically permissible. Thus, the indirect transition threshold, $h\upsilon_i$ (o), is the energy required to raise an electron from the top of the valence band at the surface of the sample to the vacuum level and is, by definition, the photoelectric threshold. That is,

$$h\upsilon_i\ (o) = E_d + \epsilon_c\ (\overline{k}_\varphi) = \Phi \qquad (2.32)$$

$\overline{k}_\varphi$ is defined as the value of $\overline{k}$ along the direction of orientation at which the vacuum level intersects the C band. The direct photoelectric threshold is the energy required to raise a valence electron at $\overline{k} = \overline{k}_\varphi$ into a state of the same $\overline{k}$ in C band by neglecting the $\overline{k}$ vector of the photon. This is

$$h\upsilon_d(o) = E_d + \epsilon_c(\overline{k}_\varphi) + \epsilon_v(\overline{k}_\varphi) = h\upsilon_i(o) + \epsilon_v(\overline{k}_\varphi). \qquad (2.33)$$

Thus, the direct photoelectric threshold energy for the photoemission is larger than the indirect threshold energy.

When the photoemission current is observed by increasing the photon energy, the current should rise slowly as the photon energy reaches the indirect photoelectric threshold, and then it should rise abruptly as the photon energy reaches the direct photoelectric threshold. Further increase of the exciting photon energy, the photocurrent will be dominated

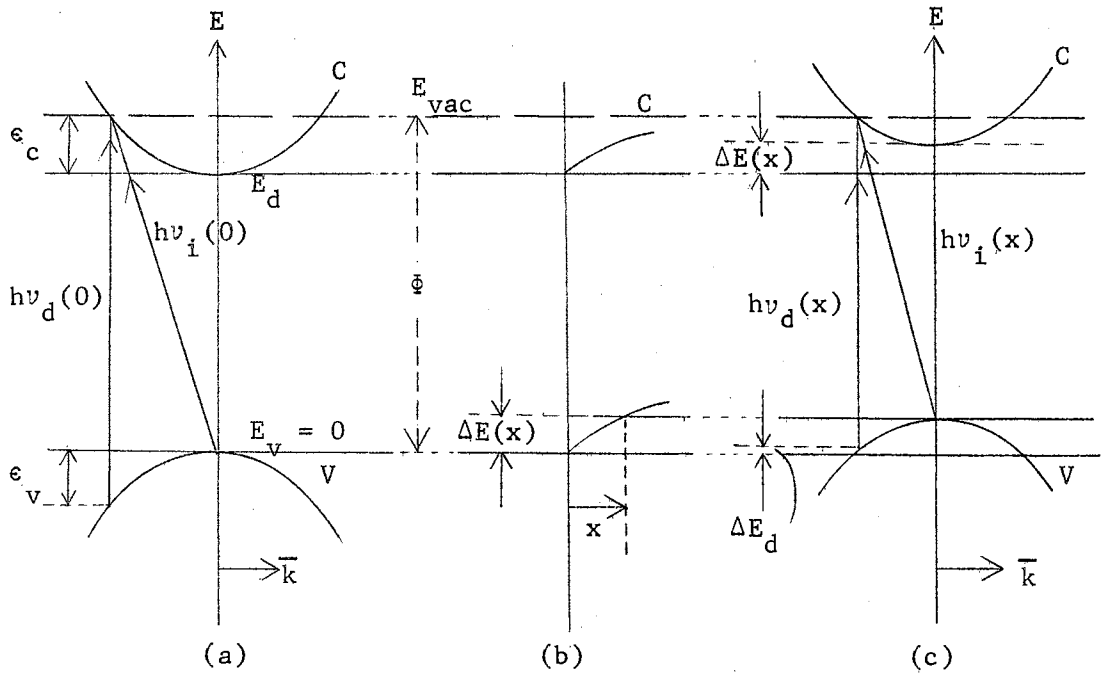

Fig. 5. Energy versus $\bar{k}$ and energy versus distance diagram for a simple two-band semiconductor

by the direct transitions of the photoelectrons. Therefore, the total emission can be written as

$$y = C_i[h\upsilon - h\upsilon_i(o)]^{5/2} + C_d[h\upsilon - h\upsilon_d(o)], \qquad (2.34)$$

where C_i and C_d are constants containing the light intensity and the absorption coefficient for the production of photoelectrons.

Consider now the effect of the depth beneath the surface at which photoelectrons are produced. We are particularly interested in the case in which the energy bands bend downward from the interior to the surface for this is the situation which exists at the surface of a semiconducting diamond (32). As shown in Fig. 5(b), the bands at a distance x beneath the surface are shifted $\Delta E(x)$ upward toward the vacuum level, and the corresponding values of the quantities $h\upsilon_i(x)$ and $h\upsilon_d(x)$ shown in Fig. 5(c) for the photoelectric emission are obviously smaller than the values of the corresponding quantities $h\upsilon_i(o)$ and $h\upsilon_d(o)$ for $x = 0$.

In evaluating the yield, the attenuation of the light and the escape depth of the exciting electrons must be considered. They are both exponential in nature. When L_α and L_e are the absorption length and escape length respectively, an expression for the photoemission is

$$y(h\upsilon,x) = C_i[h\upsilon - h\upsilon_i(x)]^{5/2}\exp(-x/L) + C_d[h\upsilon - h\upsilon_d(x)]\exp(-x/L), \tag{2.35}$$

where

$$L^{-1} = L_\alpha^{-1} + L_e^{-1}. \tag{2.36}$$

Theoretical calculations from such a model fit very well to the experimental curves on silicon.

CHAPTER III

EXPERIMENTAL METHODS

Sample Description

Two natural diamond samples were used for the external photoelectric effect measurements. The first one is a 0.863 carat rectangular parallelpied Type IIb diamond having dimensions 2.5 x 3.5 x 6.5 mm^3 and is designated as DS-2. One end of the diamond has a distinct blue color, while the other end is nearly free from coloration. Room temperature resistivity measurements are 3.6×10^5 ohm-cm for the clear end and 65 ohm-cm for the blue end. A picture of the sample is shown in Fig. 6. Its surfaces are flat; the large faces are very nearly (111) faces. Various electrical, optical and magnetic investigations for this sample have been taken previously. These include optical absorption (33, 34, 38), photoconductivity (35, 36, 38), Hall coefficient (38), minority carrier lifetime (37), rectification and photovoltaic effect (36), phosphorescence and birefringence (34), luminescence (39) and electron spin resonance (40). Hall coefficient measurements show p-type conductivity. Other measurements of the electrical, optical and magnetic properties of this sample are found in the report "Investigation of Semiconducting Properties of Type IIb Diamonds" of this laboratory, May, 1962 (32).

The second sample, designated as DS-5, is a 3.69 carat dark-blue semiconducting Type IIb diamond. There are two parallel flat faces

which were identified as (111) faces by X-ray analysis. The distance between these two faces is about 4.5 mm. The shape is irregular, with measurements along the other two sides of approximately 6 mm and 10 mm respectively. The picture of DS-5 is shown in Fig. 7. The largest face is one of the (111) faces on which photoelectric emission was observed. Resistivity, measured between two flat surfaces, is estimated at less than 100 ohm-cm.

A germanium sample, Ge-1, was also prepared for the photoelectric emission measurements. The germanium crystal was doped with antimony, having n-type conductivity of 2.2 ohm-cm. It was drawn by the Teal-Little technique along the <111> direction. The sample was a part of a thin slice which was cut out of the crystal in a direction perpendicular to the axis. The size of the sample was 6.5 x 9.0 x 0.70 mm^3, with its large surfaces being (111) faces.

Sample Cleaning and Mounting

Both samples DS-2 and DS-5 were cleaned with aqua regia (82 parts HCl, 18 parts HNO_3 by volume), and HF by soaking them for two hours in each of the solutions. Most impurities, as mentioned earlier, will have been dissolved if they happened to exist on the surface of the crystal. The samples were degreased with carbon tetrachloride, and rinsed with acetone, distilled water and iso-propanol before making electrical contact. The contacts to both crystals were made to the surface of the (111) face by directly soldering it with a solder consisting of 3% indium and 97% 40-60 tin-lead solder. The use of indium is to avoid the formation of a p-n junction. In doing this soldering, each diamond was first placed on a hot plate and evenly heated to about

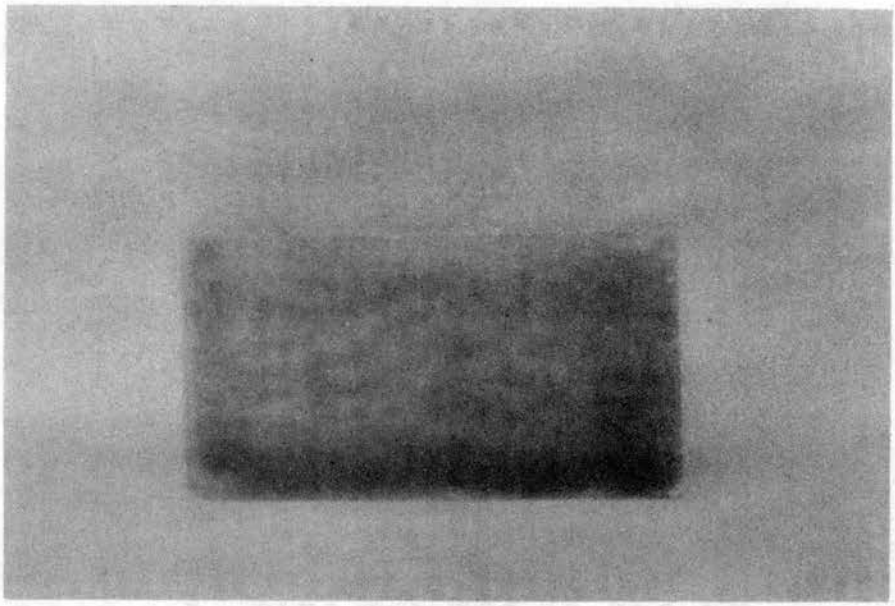

Fig. 6. The diamond DS-2

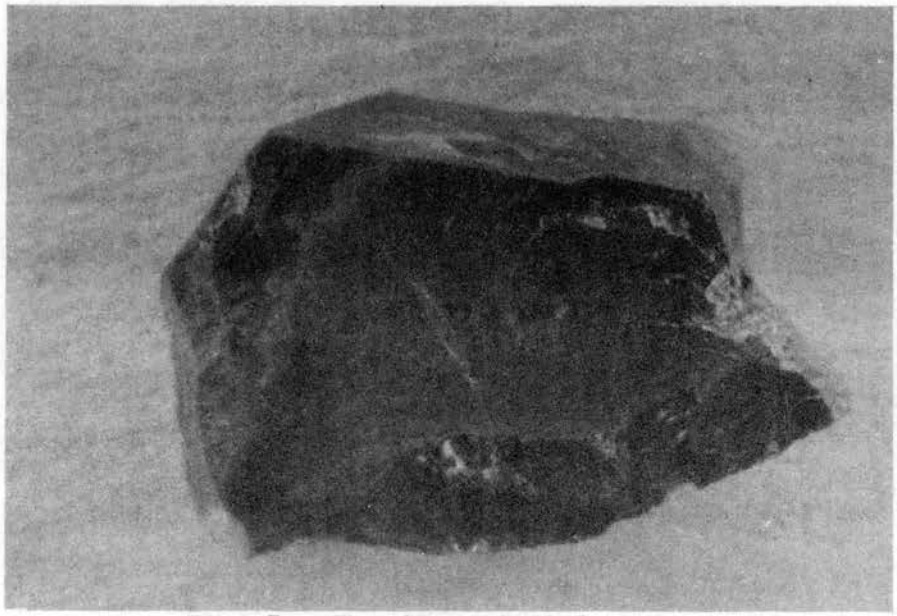

Fig. 7. The diamond DS-5

350° C before the soldering iron was applied. The soldering iron is rated at 22.5 watts and generates about the same temperature. By twisting the melted solder over the surface of the diamond, the solder was spread on it. In making an electrical lead, a tinned copper wire of one millimeter in diameter was attached to the melted solder. The diamond was then allowed to cool gradually with the copper wire kept at a proper position. The contact was found satisfactory electrically and solid mechanically.

After the electrical lead connections were made, the sample DS-2 and the connecting wire were again degreased and washed in the same manner. The process of cleaning for sample DS-5, after making electrical connection, was somewhat different. The sample DS-5 with the connecting wire was washed twice in boiling distilled water to remove the flux. It was then rinsed with distilled water and iso-propanol. Final cleaning was given to the diamond by inserting it in a vapor degreasing flask working with iso-propanol for 100 minutes. The residual moisture on the surface immediately evaporated after it was removed from the flask due to its own temperature.

Figure 8 shows the sample DS-2 mounted to a sample holder. The copper wire served as an electrical lead and supporter. It was put into a quartz sleeve with its free end soldered to another wire which was glass-metal sealed into the center of the Pyrex stopper. The metal parts and the top of the stopper were painted with polystyrene. Both the quartz tubing and the polystyrene were used for protecting spurious emission from the scattering light.

In Fig. 9 is shown the sample assembly for DS-5. It was prepared specifically to fit into a second photoelectric cell which will be

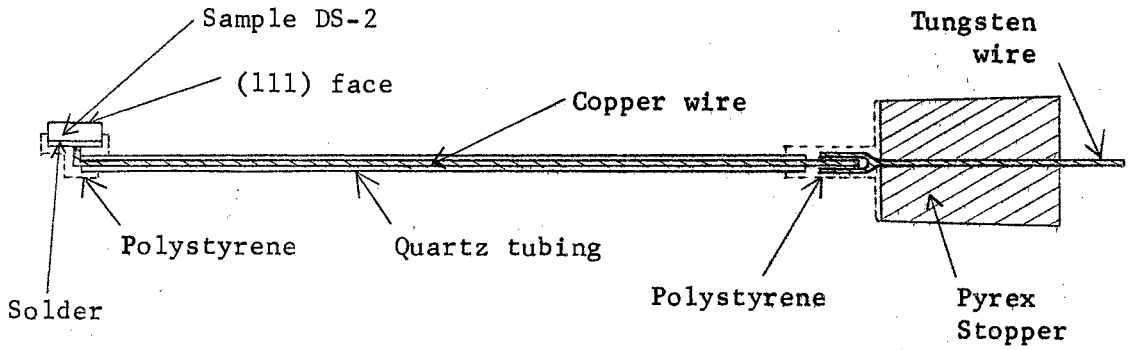

Fig. 8. Sample assembly for DS-2

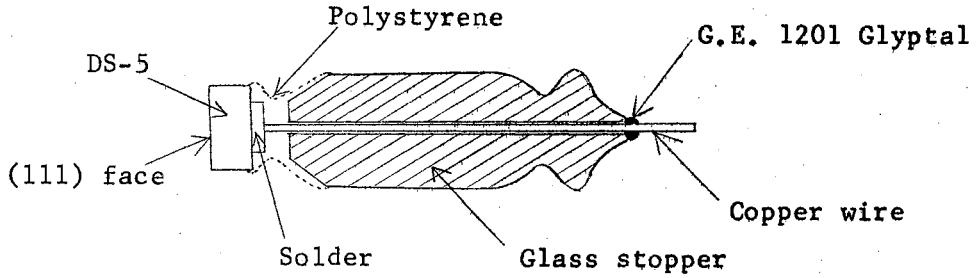

Fig. 9. Sample assembly for DS-5

described later. After final washing, the connecting wire was sealed into the matched hole at the center of the glass stopper with General Electric 1201 red enamel Glyptal. The solder, copper wire, and the top of the glass stopper were then painted with the same polystyrene. The assembly was then placed in an electrical oven for drying.

The germanium sample was etched with CP-4 etchant (20 parts HNO_3, 12 parts HF, 12 parts acetic acid, 0.5 parts Br_2 by volume). After etching, it was rinsed with distilled water, acetone and iso-propanol. Electrical contact was made with regular 40-60 ratio tin-lead solder. The washing was repeated after the contact was made. The sample was then mounted to a sample holder in the same way as DS-2 (Fig. 8).

Photoemission Tube

Photoemission cells were constructed for the measurements of the photoelectric emission. In this type of cell, electrons are ejected from a surface, the cathode, by the action of light, and are collected by a second electrode, the anode. The latter is usually maintained at a positive potential by an external battery. An ideal geometry of a photoemission cell is a hollow sphere having a conductive layer coated on the inner surface to act as the anode and having a point cathode placed at the center of the sphere. Such a geometry allows a symmetrical field to act upon the electrons emitted equally from all directions.

For practical purposes, the two photoelectric cells designed were not spherical. The photoelectric cell shown in Fig. 10 was made of a five-inch long Pyrex tube one inch in diameter. The inner wall of the cell was completely silvered, and the conducting surface acted as the anode. Light was allowed to fall into the cell through an aperture one

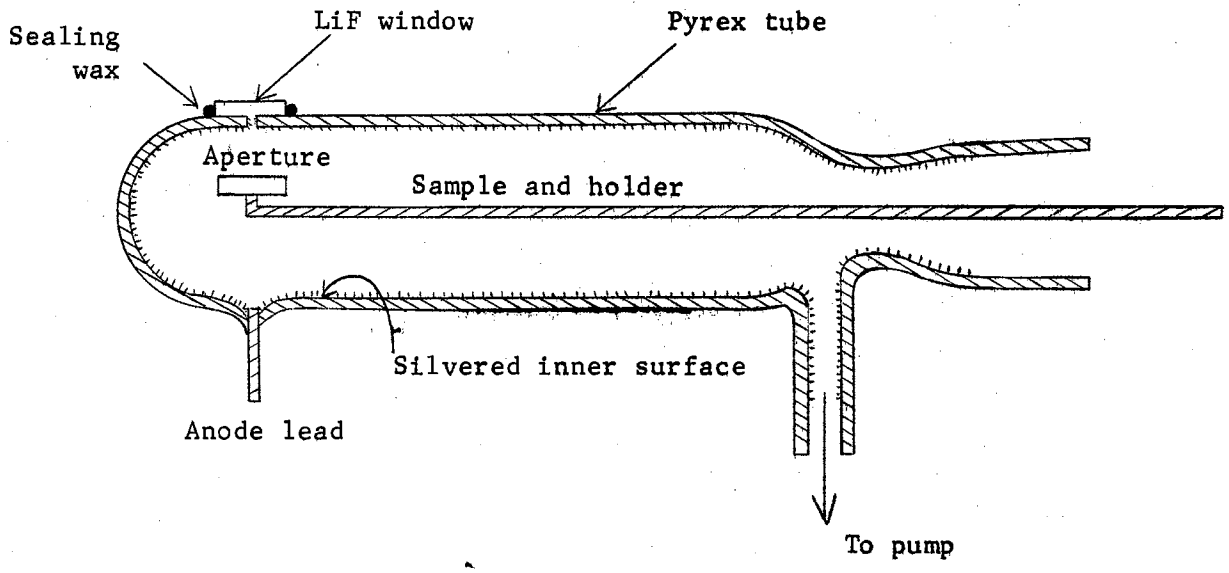

Fig. 10. Sketch of photoemission cell for DS-2

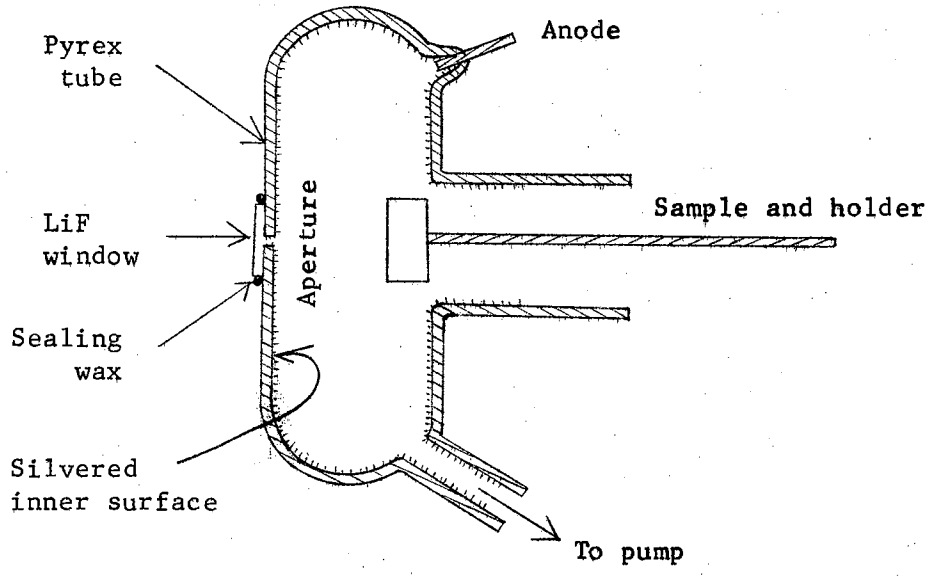

Fig. 11. Sketch of photoemission cell for DS-5

millimeter in diameter. The aperture was covered with a LiF window which was sealed to the glass with General Electric 1201 red enamel Glyptal and Apiezon wax. The seal was checked for leaks before the sample DS-2 was put into the tube. The stopper was sealed to the tube by using the same Glyptal. The length of the sample holder was measured in advance so that the center of the diamond surface was directly below the aperture after final sealing. The distance between the aperture and the diamond surface was kept small so that the incident light passing through the aperture would fall completely onto the diamond surface. A long sample holder was provided in order to minimize the spurious emission from the stopper by the action of scattered light. The photoelectric cell was also used for housing the germanium sample Ge-1.

In Fig. 11 is a sketch of the photoelectric cell which was designed for housing the larger diamond sample DS-5. This photocell was also made from a Pyrex tube. In order to avoid exposure of the long sample holder to the scattering light the photocell was constructed with a short sample holder, but its structure differs from the other photocell only in geometry. The sample assembly was sealed into the tube by the same method after the final cleaning. Care was taken to place the diamond surface, the (111) face, directly below the aperture of the photocell at a short distance from it. The thickness of the LiF windows in both photocells was 0.80 mm.

Light Source

A light source which is rich in extreme ultraviolet light may be a vacuum spark, a hydrogen discharge tube, or an electric arc operated in a gas which is transparent to the extreme ultraviolet light.

A vacuum spark light source was set up within a large vacuum chamber of a vacuum coating unit. It was operated at a pressure of 10^{-5} mm of Hg by connecting a transformer across the electrodes. The transformer was manufactured by General Electric; it has an output of 12,000 volts at 24 ma. The capacitance in parallel with the secondary of the transformer varied between 800 and 1200 μμf. Electrodes made from iron, zinc, aluminum and carbon were tested. The vacuum sparks were intermittent and unstable in nature and were apparently very weak because of the rather small power of the transformer.

A few gases are transparent to light in the extreme ultraviolet region so that a light source consisting of an electric arc discharged in a gas was set up for operation. Among the few kinds of electrodes used in the electric arc, a carbon arc was found to be rich and intense in radiation in the short wavelength region. The development of a light source having a carbon arc operated in a pure gas was then undertaken.

The electrode assembly of the carbon arc is shown in Fig. 12. The carbon rods were manufactured by National Spectroscopic Carbons of the National Carbon Company. The diameter of the rods was one-eighth of an inch. One end of each rod was shaped like the tip of a ball pen before it was fitted into the glass sleeves. Each end extended out of the sleeve about one half of one millimeter; the ends were set about one millimeter apart. The electrodes were housed and supported with a glass bulb which was one inch in diameter at the middle portion and six inches long. At the middle of the glass bulb an opening was provided for the passage of the light. The sleeves of the electrodes limited the spreading of the arc, thus enhancing the intensity of the light source. The glass bulb prevented the spreading of the charged

particles which evolved from the thermal emission of the carbon arc.

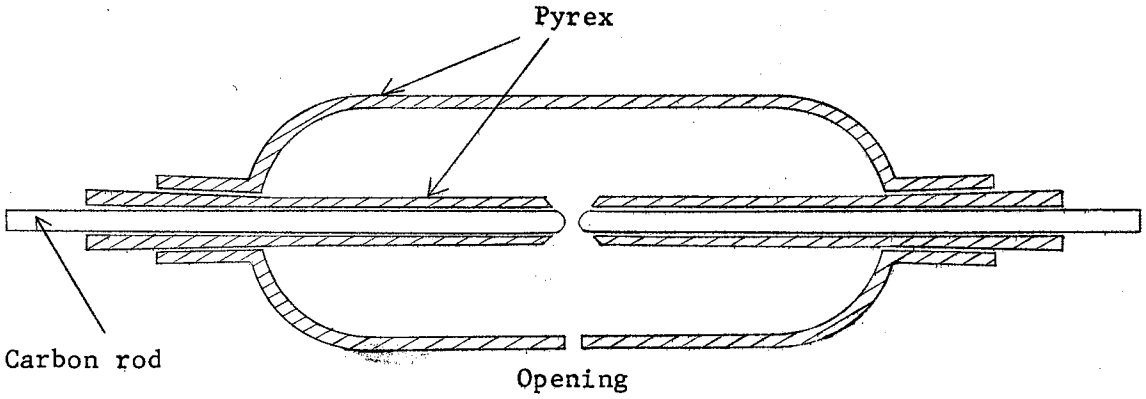

Fig. 12. Electrode assembly.

The carbon electrodes were connected to the secondary of a power transformer. The transformer, Type T-7351, was manufactured by Thordarson Electric Company and was rated at 1300 VA. It provides 4300 volts and 1900 volts. When 4300 volts was applied to the electrodes by having a ballast resistor in series with the primary, the arc current was limited to approximately 350 ma.

The carbon arc was set up within a large vacuum chamber over the base plate of the same vacuum coating unit mentioned earlier. Details of this unit will be given later. The high voltage leads of the transformer were first brought to the glass insulated high voltage connectors which extended from the bottom to the top of the base plate of the vacuum chamber; electrical connections were then made between the glass insulated connectors and the carbon electrodes in the chamber. The glass insulated connectors were one half of an inch in diameter and were sealed with O-rings to the plate.

The carbon arc was examined by operating it in air, in a reduced pressure of dry helium gas, and dry nitrogen gas. In the discharge of the carbon arc in air, the electrodes were found to burn away in a few seconds; this weakened the light source. Nevertheless, the intensity of light in the range of short wavelengths was fairly high upon applying 4300 volts across the electrodes.

When the discharges of the carbon arc in helium gas were examined at a pressure from a few millimeters to 157 mm of Hg, a glow discharge was always observed in the surroundings of the electrodes.

By discharging the carbon arc at 4300 volts in nitrogen gas, a glow discharge was found at a pressure from a few millimeters to 38 mm of Hg, but it disappeared completely at a pressure of 41 mm of Hg. The carbon arc operated in a reduced pressure of nitrogen gas and was not very stable because of the slow burning away of the electrodes; however, it was found satisfactory in regard to the wavelengths, intensity, and the continuation of arcing of the radiation.

In the following measurements the carbon arc was operated at 4300 volts either in air or in a reduced pressure of nitrogen gas. In the latter case, the chamber in which the electrode assembly was placed was first evacuated to a vacuum of 2×10^{-4} mm of Hg and then filled with nitrogen gas. The pressure of the nitrogen gas was then maintained at 110 mm of Hg as it was measured with a mercury manometer. It should be mentioned that the photoelectric emission current from the diamond was extremely feeble when discharging the carbon arc at 1900 volts.

Optical Filters

In the region of extreme ultraviolet light, filters are quite

limited. Some materials commonly used for windows are also used as filters. The short wave limit of transmission of some crystal filters and some liquid filters that are of interest to us is given in Table I. The accuracy of the values will depend upon the criteria used; some were referred to ten per cent transmission, while others could have been twenty per cent transmission. The thickness, the purity, and the surface conditions of the material also effect transmission. In the filters being used, the surfaces of the sapphire, quartz and Corning Glass filters were well polished by the manufacturers. The surfaces of halide filters were either cleaved or polished on soft cloth with Linde grade A polishing compound wetted with iso-propanol or butyl alcohol (41). When it was necessary to hold the crystal in the fingers, rubber finger cots were used.

TABLE I

OPTICAL FILTERS

Filter	Short Wavelength Limit (Å)
LiF (10)	1050
CaF_2 (10, 42)	1230
SrF_2 (10)	1280
BaF_2 (10, 42)	1350
Sapphire (10, 44)	1420
Cultured fused quartz (10, 43)	1450
Fused silica (10, 45)	1600 - 1850
NaCl (46)	1900
Distilled water, 2 cm (47)	2000
KCl (48)	2026
KBr (48)	2063
NaBr (48)	2100
Corning Glass 9741	2100
Corning Glass 7910	2250
Ethylether 1 cm (49)	2250
Methy alcohol, 2 cm (47)	2300
Ethyl alcohol, absolute, u.w.p., 2 cm (47)	2350
CsI (1.5 mm) (50)	2420
KI (45, 48)	2500
Cyclohexane, pure, Eastman Kodak Co., 2 cm, (47)	2650
Carbon tetrachloride, 1 cm (49)	2700

Vacuum Systems

Two vacuum systems were employed in the photoelectric emission measurements. The first one was used for evacuating the photoelectric cell in which ultrahigh vacuum was desirable. This system consisted of a fore pump and three stage fractionating oil diffusion pump. The fore pump was the Welch Scientific Company's Duo-Seal No. 1405 vacuum pump. The diffusion pump was constructed with Pyrex glass equipped with a cryogenic trap. In order to obtain an ultrahigh vacuum, a low vapor pressure Apiezon N grease was used for the glass stoppers. Octoil of Consolidated Vacuum Company was used for the pump fluid of the diffusion pump. The octoil in the diffusion pump was continuously purified. The most volatile components derived from the pyrolysis of the oil were distilled directly into the depression on the cooling wall of the last stage, the components of the intermediate vapor pressure formed the vapor stream, and the tarry residue was collected in an extra boiler. A cold cathode ionization gauge, Model 100A of Miller Laboratories, was used for measuring the high vacuum. The gauge has a panel meter with gradual ranges from 10^{-3} to 10^{-7} mm of Hg. A pressure of 2×10^{-8} mm of Hg corresponds to a division of 1.2 mm wide which is clearly readable.

The second vacuum system was a Type LC1-14B Laboratory Vacuum System manufactured by Consolidated Vacuum Company. It was mounted in a cabinet 37 inches wide and 32 inches deep. The chamber was a Pyrex glass bell jar covering over a circular stainless steel base plate. The jar had a diameter of 14.25 inches, a usable inside diameter of 13.25 inches and a height of 24 inches. The base plate contained an inlet port, a hole for mounting the sensing tube of the discharge gauge, and

twelve holes of 3/4 inch diameter for introducing gas, and electrical connectors into the chamber. The fore pump was a Welch Scientific Company's No. 1397 vacuum pump. The diffusion pump was Type PMC-720 of the same company.

The Electrometer

Electronic charges collected by the anode of the photoelectric cell were measured with a Cary Model 31 vibrating reed electrometer purchased from Applied Physics Corporation. It consisted of two units, the electrometer head and the amplifier cabinet, which were joined by a cable with multiple connections. The vibrating reed electrometer is characterized by the fact that mechanical energy is used to move the impressed charge in an electrostatic field. Mechanical energy is thereby transformed into electrical energy, an ac signal. The ac signal is amplified, rectified, and then used to drive an indicating meter.

The general principle of operation is as follows: When a quantity of charge is placed on a condenser, the condenser is charged to a potential. If the capacitance of the condenser changes a small amount, it introduces a change in potential. If the capacitance of the condenser is varied periodically by setting the condenser in vibration, then a periodic voltage is generated across the condenser. The ac voltage is a function of the impressed charge, the capacitance and the variation of the capacitance of the condenser. The ac voltage is thus a measure of the impressed charge. Details of the principle are given by Palevsky, Swank and Grenchik (51).

In the measurement of the small current, a high value standard resistor was connected between the input and the feedback terminals of

the electrometer. The steady deflection shown by the meter corresponds to the input photoelectric emission current flowing across the standard resistor. A set of three standard resistors was provided in the electrometer by using a turret switch. The resistors were 1.0×10^{10}, 1.0×10^{11} and 1.0×10^{12} ohm and were marked in the order of 2, 3, and 4 respectively on the switch.

The panel meter is a four-inch scale which indicates the quantity of charge on the electrometer. The ranges are provided corresponding to 1, 3, 10, 30, 100 and 300 mV and 1, 3, 10, 30 and 30 volts full scale. Current can be measured in the range between 10^{-9} and 10^{-16} ampere. The stability is less than 5×10^{-17} ampere.

Arrangement of Apparatus

The block diagram for the arrangement of the apparatus is shown in Fig. 13. The double lined block indicates the vacuum chamber. As stated earlier, the electrode assembly of the light source was placed over the base plate of the vacuum chamber. The leads of the electrodes were brought out through glass insulated connectors to the transformer. The photoelectric cell was also placed in the chamber so that its window directly faced the carbon arc a few centimeters away. Electrical connections from the electrodes of the photoelectric cell were brought out of the chamber from the base plate in the same manner by using glass insulated connectors. Two other holes provided at the base plate were separately used for evacuating the photocell through the three-stage oil diffusion pump and for admitting nitrogen gas to the chamber.

The electrode from the sample was connected to the input post of the electrometer at the center of the head unit. The collecting electrode

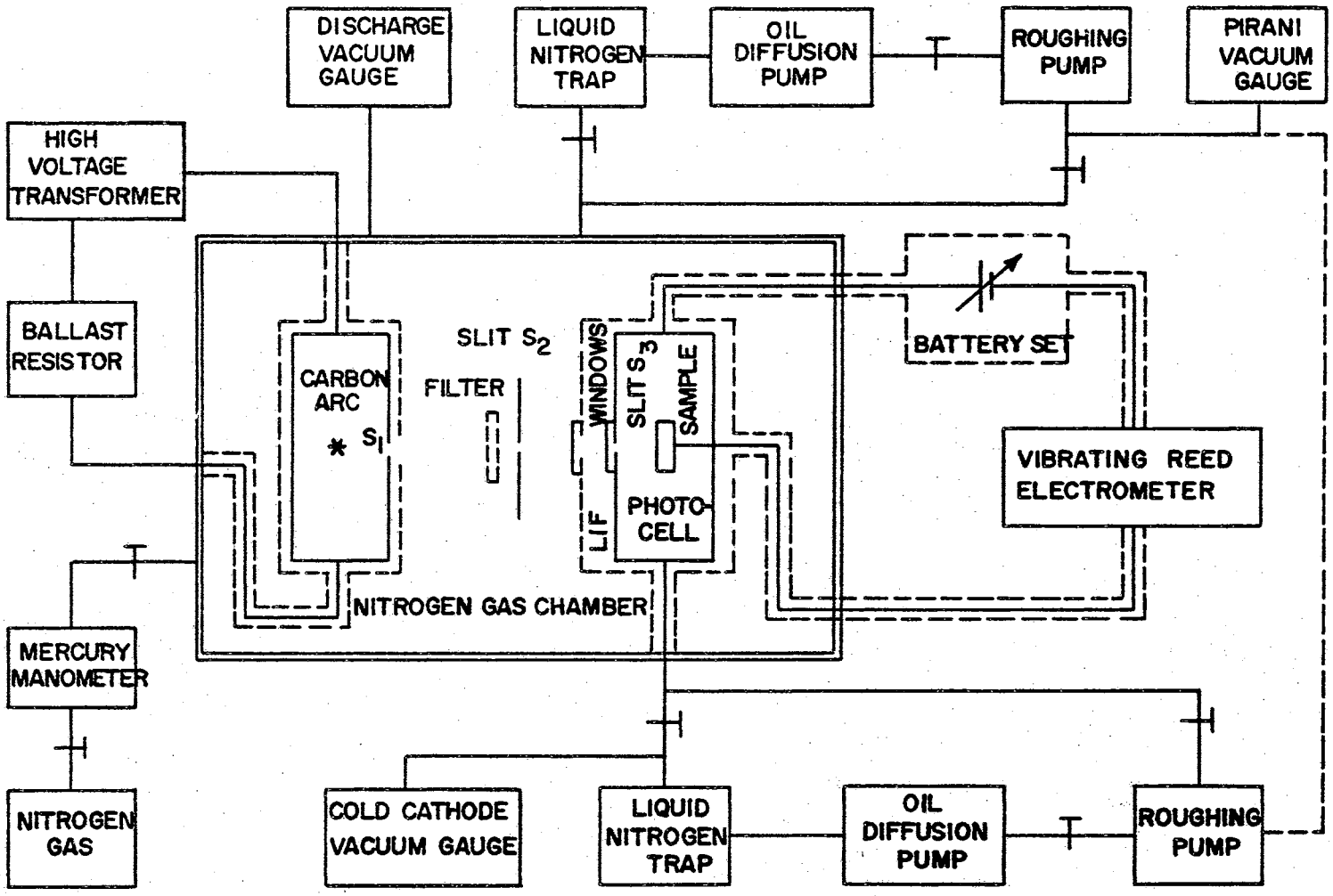

Fig. 13. Block diagram of photoemission apparatus

was connected to the positive side of a battery. The other side of the battery was connected to the feedback terminal of the electrometer. A different potential of the collecting electrode was obtained by the bias connection shown in Fig. 14. The carbon electrodes and the glass insulated connectors were covered with a grounded tin plate box to isolate the electrostatic field effect. The photocell, the battery set, and the electrometer head unit were also placed separately into grounded tin plate boxes used for the purpose of shielding. Because of the small photocurrent flowing in the circuit the shielding of the connecting wires was extremely important; therefore, all the wires were triply shielded. This is indicated in the diagram by dashed lines.

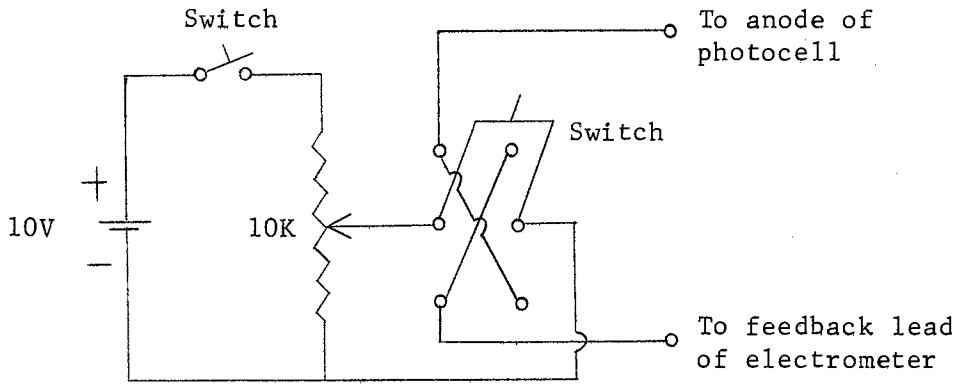

Fig. 14. Collector bias connection

The aperture of both photocells S_3 is as shown in Fig. 13. Another slit S_2 was placed directly behind the tin plate box of the carbon arc. The LiF window attached to the tin plate box of the photocell was used to prevent the charged particles emitted from the heated carbon electrode from drifting to the electrical leads of the photocell.

In the measurements for diamond DS-2, the distance between the opening of the carbon arc enclosure and slit S_2 was 0.65 cm and that between slit S_2 and slit S_3 was 2.4 cm. S_3 was set at 1.0 cm from the sample. In the measurements for diamond DS-5, the corresponding distances were 0.5, 2.64 and 1.0 cm, respectively. In both cases, the diameter of slit S_3 was 1.0 mm. The diameter of slit S_2 was set at 2.0 mm in the measurements for diamond DS-2 and at 1.32 mm in the measurements for diamond DS-5. The measurements for germanium sample Ge-1 were similar to those for diamond DS-2 with diameter of slit S_2 varying from 0.7 mm to 2 mm.

CHAPTER IV

EXPERIMENTAL RESULTS

Photoelectric Emission from Diamond DS-2

Three sets of data were taken for this sample. In the first and second sets, the photoelectric emission currents were observed by varying the potential of the collecting electrode from positive four volts to negative five volts. Although the saturation emission current was generally reached below two volts, the value varies with the geometry of the photocell, the energy of the exciting photons and the work function of the metal acting as a collecting electrode. The measurements in each set were taken first without any filters. This allowed the light to fall on the sample only after passing through the LiF windows. The LiF windows absorbed all the light having wavelengths shorter than 1050 Å and transmitted part of the light having wavelengths longer than the 1050 Å. Different extents of wavelengths of the incident light were obtained by using crystal or liquid filters.

The first set of data was taken with a freshly cleaned sample surface with the photocell maintained at a pressure of 10^{-3} mm of Hg. The second set of measurements was taken on an aged sample surface with the photocell maintained at a pressure of 10^{-8} mm of Hg. The photoelectric emission current-potential characteristics in these two sets of measurements are given in Figs. 15 and 16; each curve obtained with a specific filter is indicated. The saturation currents which resulted

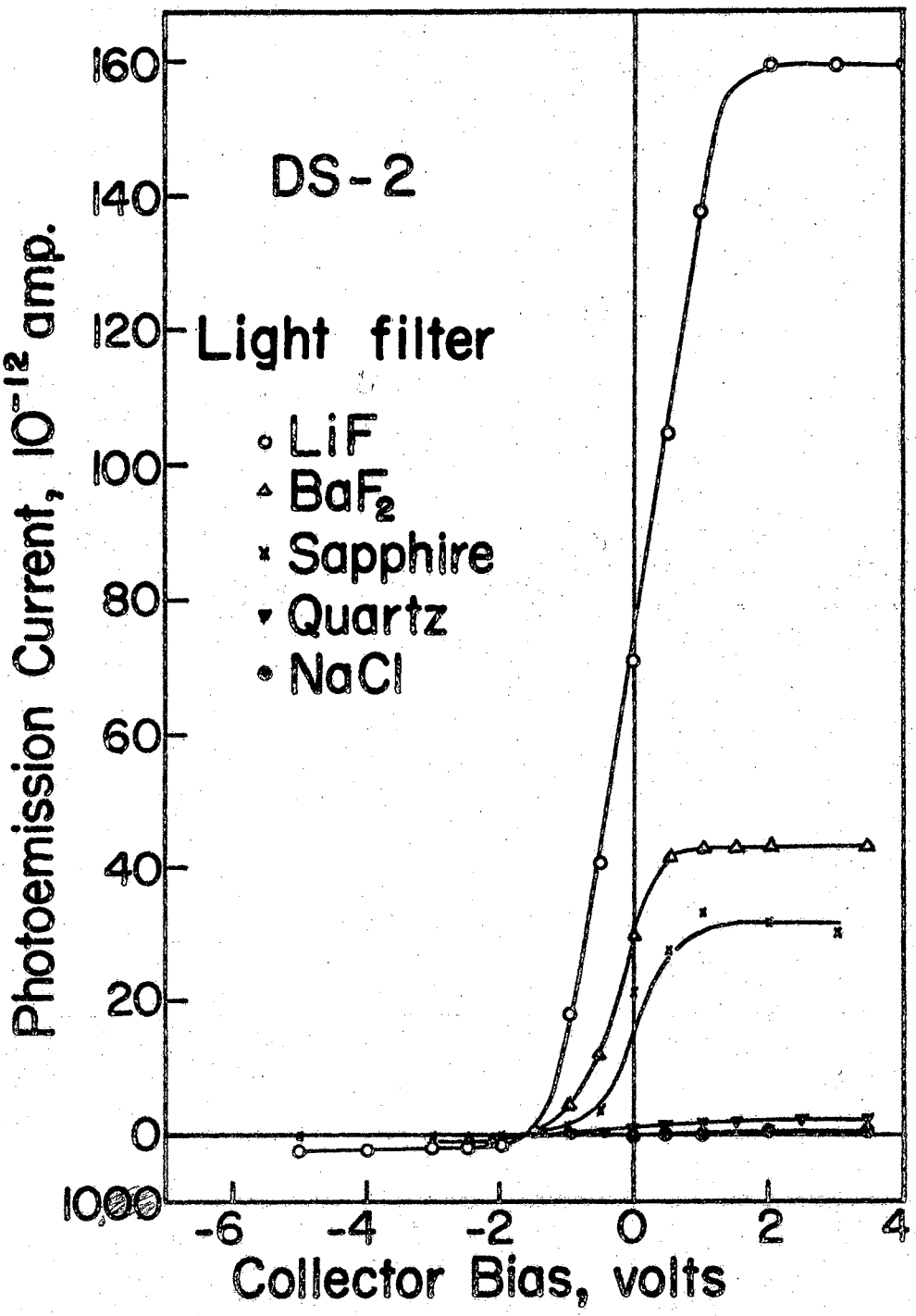

Fig. 15. Photoemission current-potential characteristics for diamond DS-2. (I)

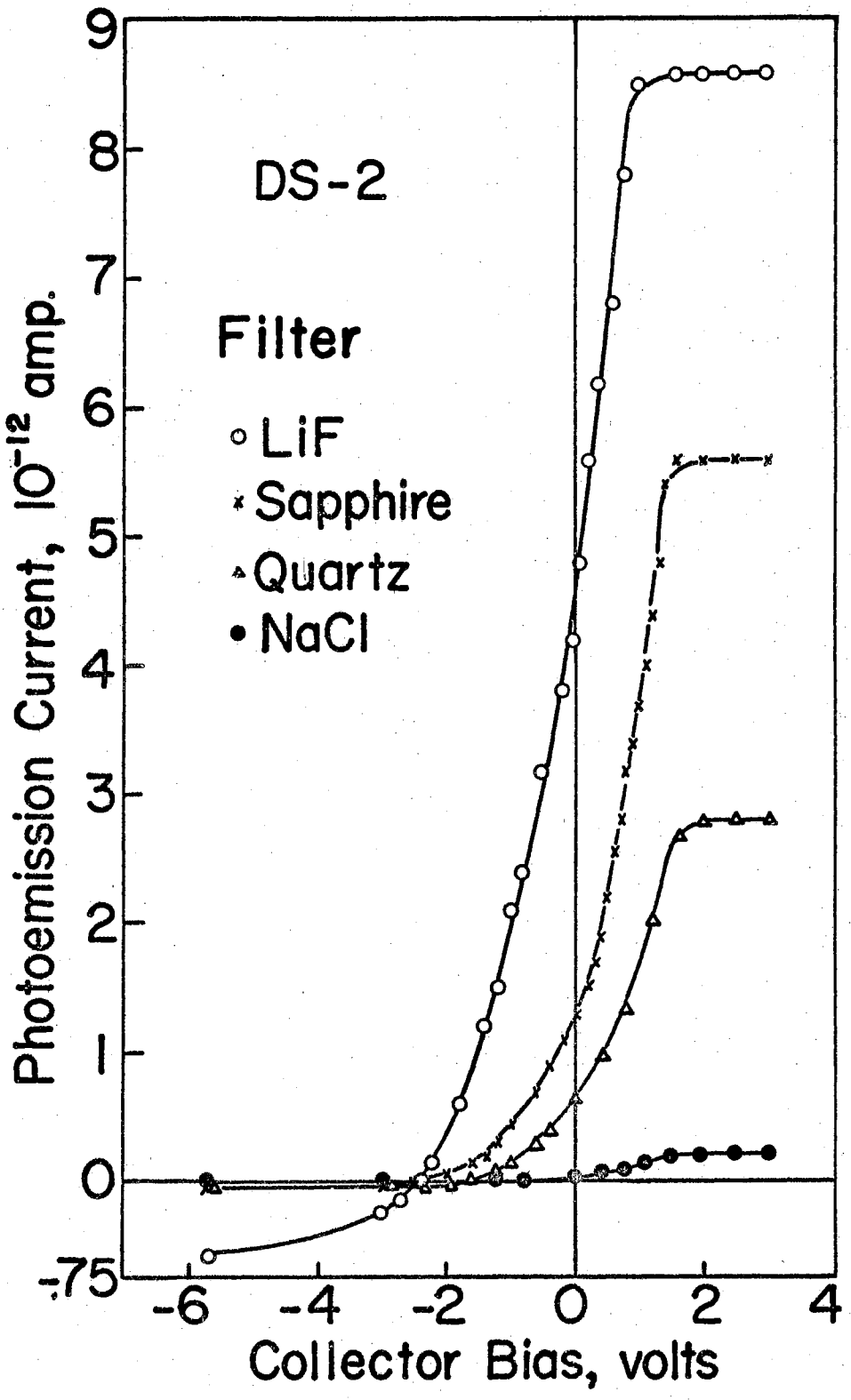

Fig. 16. Photoemission current-potential characteristics for diamond DS-2. (II)

from using various filters are tabulated in Table II and Table III. In the second column of these tables is the short wavelength limit which may vary somewhat with the thickness of the filters. The spectral distribution of the emission is presented in Figs. 17 and 18.

TABLE II

SATURATION PHOTOEMISSION CURRENT FROM DIAMOND DS-2. (I)

Window or filter (mm)	Short wave length limit (Å)	Maximum photon energy (eV)	Saturation current (10^{-14} amp.)
LiF (1.6)	1050	11.8	1600
BaF_2 (1.6)	1350	9.17	430
Sapphire (0.50)	1420	8.74	340
Quartz (4.0)	1700	7.30	160
NaCl (4.4)	1900	6.52	24

TABLE III

SATURATION PHOTOEMISSION CURRENT FROM DIAMOND DS-2. (II)

Window or filter (mm)	Short wave length limit (Å)	Maximum photon energy (eV)	Saturation current (10^{-14}amp.)	Reverse current (10^{-14}amp.)	Photocell pressure (10^{-8}mm Hg)
LiF (1.6)	1050	11.8	860	-55	3
Sapphire (0.50)	1420	8.73	540	-1.8	5
Quartz (4.0)	1700	7.30	280	-1.4	5
NaCl (1.3)	1900	6.52	15	+0.08	2

From Figs. 15 and 16, we see that the photoemission current reached saturation when a positive bias of less than two volts was applied to the collecting electrode. The saturation current dropped drastically when the light was filtered through BaF_2 or sapphire. This indicated the presence of intense light of wavelengths between 1050 Å and 1420 Å

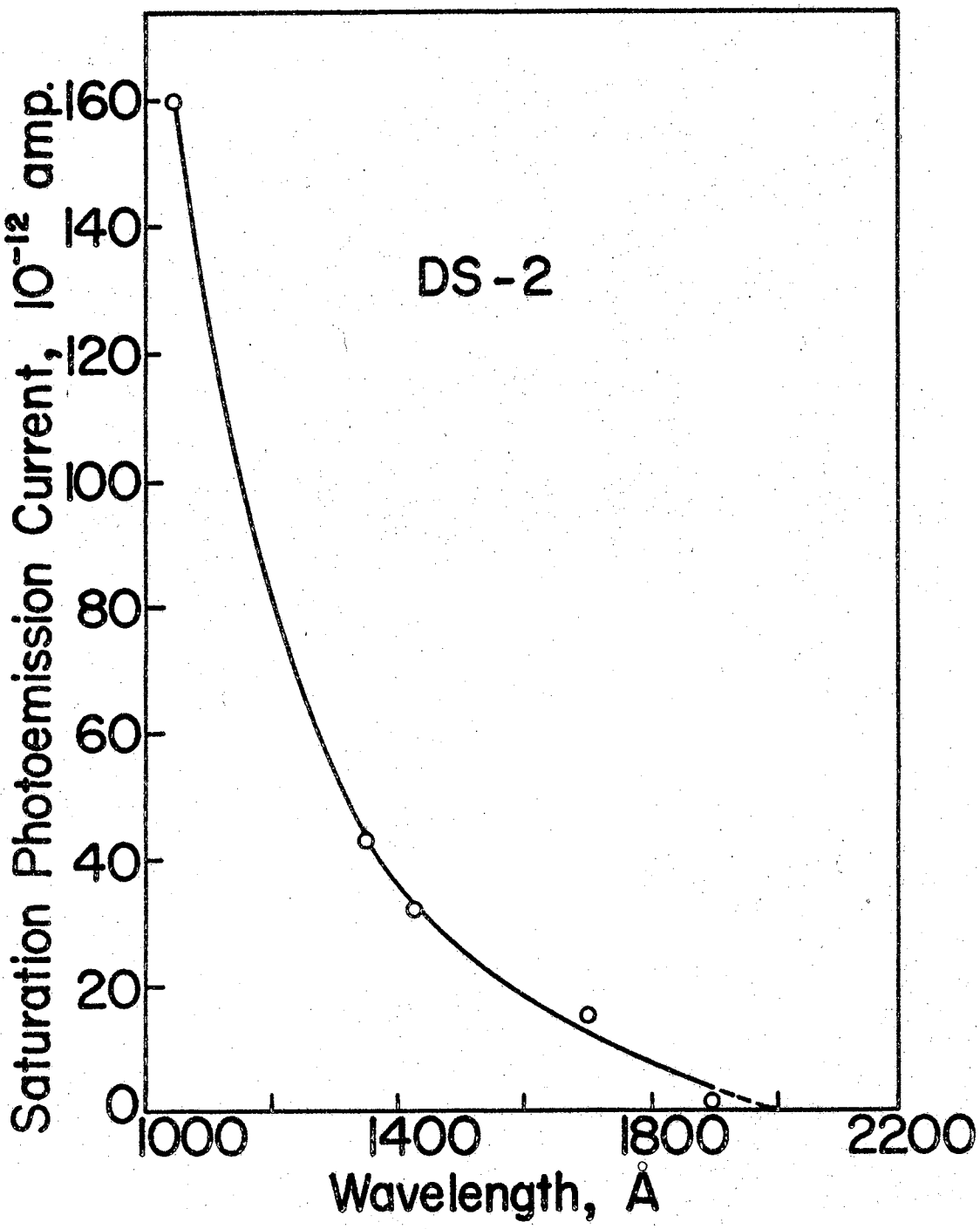

Fig. 17. Spectral distribution of the electron emission for diamond DS-2.(I)

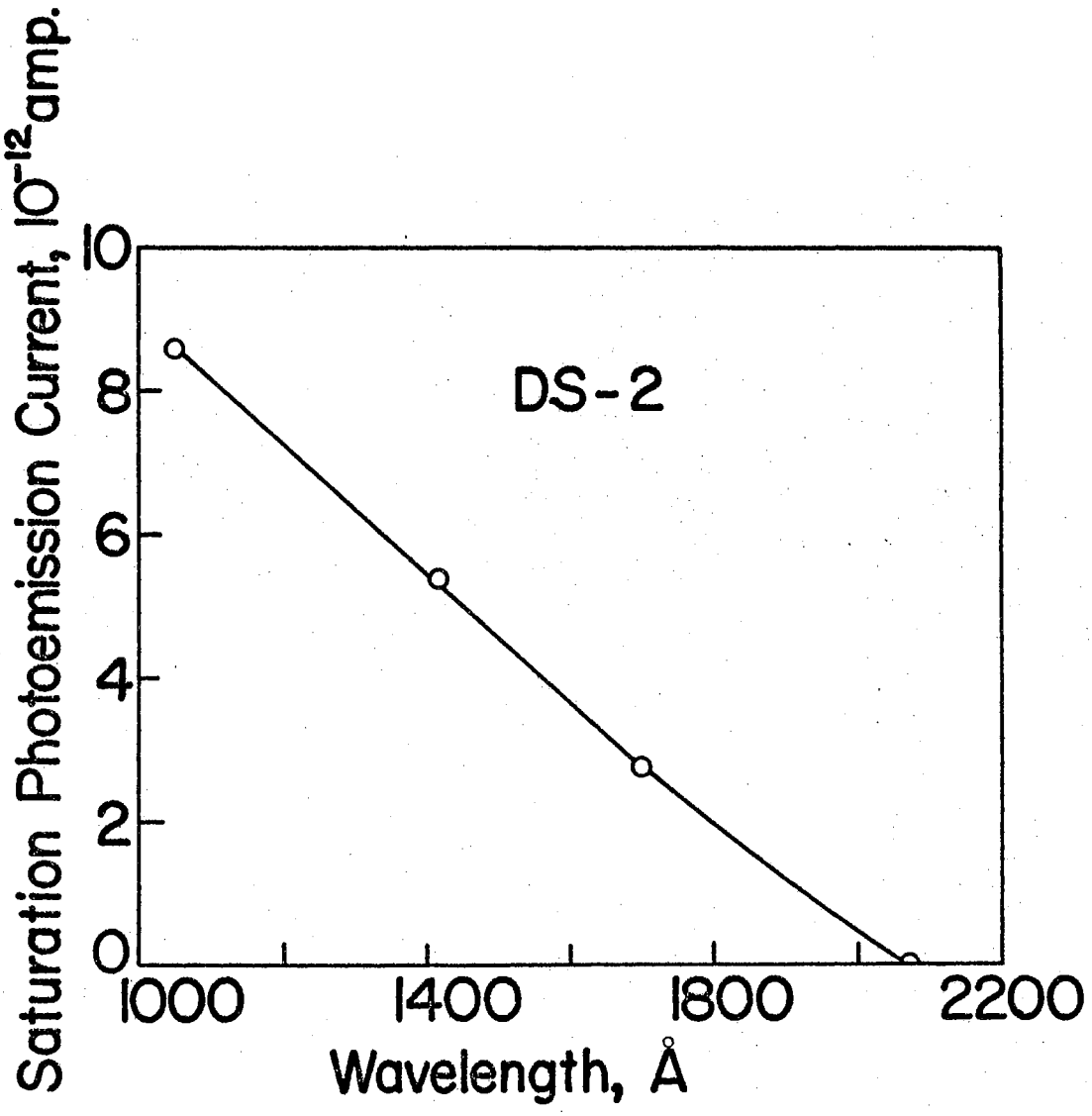

Fig. 18. Spectral distribution of the electron emission for diamond DS-2.(II)

which effectively produced the photoelectric emission. The saturation current, plotted versus wavelength of the exciting light shown in Figs. 17 and 18, dropped to almost zero when the light was filtered through the NaCl filter. The photoelectric threshold for the electron emission may be obtained by an extrapolation of the curves. They are found to be between 2000 Å and 2100 Å, corresponding to a photon energy between 6.2 eV and 5.9 eV.

Since these two sets of data were taken at a slightly different condition in regard to the distance between the slits, the intensity of the exciting light and the pressure in the photocell, the corresponding saturation currents should not be compared quantitatively. However, the fact that the freshly cleaned sample surface gave stronger photoelectric emission than the aged sample surface is obvious.

The above figures show the strong photoelectric emission from diamond with exciting light of wavelengths in the region between 1050 Å and 1900 Å. Attention was then directed to the exciting light of wavelengths at somewhat above 1900 Å in the third set of measurements. By having the light of shorter wavelengths still further filtered step by step, the threshold wavelength for the photoelectric emission was eventually determined. Since air is transparent to light of such wavelengths, it was not necessary to have the light source operated in a medium of nitrogen gas. Furthermore, the liquid filter was not sealed for use in vacuum; therefore, the carbon arc was operated in air. Except for a difference in the light source, no other changes were made in instrument arrangement. The liquid used as a filter was contained in a Beckman silica absorption cell, having a base area of 1.13 x 1.13 cm^2, a height of 4.5 cm, and a wall thickness of 0.13 cm. Liquids used were distilled water and ethyl

ether. Crystal filters include NaCl, KBr, CsI and KI. The saturation photoelectric emission currents were measured by biasing the collecting electrode at a positive five volts; the results are given in Table IV.

TABLE IV

SATURATION PHOTOEMISSION CURRENT FROM DIAMOND DS-2. (III)

Filter (mm)	Short wavelength limit (Å)	Maximum photon energy (eV)	Saturation Current (10^{-4} amp.)
Quartz cell (2.6)	1820	6.80	32.5
NaCl (1.3)	1900	6.52	15.0
Distilled water (10.01)	2000	6.20	11.8
KCl (1.6)	2063	6.02	2.5
Ethyl ether (10.01)	2250	5.52	0.5
CsI (48)	2420	5.13	0
KI (5.7)	2540	4.90	0

In Table IV, a small photoelectric emission current was observed when the incident light was filtered through ethyl ether. It is likely that this small amount of current can be attributed to the photoelectric emission of surfaces other than diamond surface by the scattering light. The photocurrent obtained by having the incident light filtered through KCl is significant. The KCl filter has a short wavelength limit at 2063 Å corresponding to 6.02 eV; therefore, the photoelectric threshold for the emission of electrons from diamond DS-2 is approximately 6.02 eV.

Photoelectric Emission from Diamond Sample DS-5

The diamond DS-5 was mounted and sealed in the second photoelectric cell. By replacing the photoelectric cell with the second one in the same arrangement of apparatus, we were ready for the investigation of

the photoelectric emissions of diamond DS-5.

Two sets of data were taken on the sample. The first set was to observe the photoemission currents from a freshly cleaned sample surface at different collecting voltages in the range of a few volts when the pressure of the photocell was maintained at 10^{-8} mm of Hg and when each of the filters was used. The carbon arc was again operated in nitrogen gas. The photoelectric emission current-potential characteristics are shown in Figs. 19(a) and 19(b); the specific filter used is also indicated. The saturation photocurrents are given in Table V where related information on the filters is also presented. When the saturation photocurrent is plotted versus the long wavelength limit of the filters, we obtained the solid line curve in Fig. 20.

TABLE V

SATURATION PHOTOEMISSION CURRENT FROM DIAMOND DS-5. (I)

Window or filter (mm)	Short wave length limit (Å)	Maximum photon energy (eV)	Saturation current (10^{-14} amp.)	Reverse Current (10^{-14} amp.)	Pressure photocell (10^{-8} mm Hg.)
LiF (1.6)	1050	11.8	1300	-80	6
CaF_2 (1.7)	1230	10.0	820	-40	3
Sapphire (0.50)	1420	8.74	640	-26	7
Quartz (4.0)	1700	7.30	155	-7.5	9
NaCl (1.3)	1900	6.52	54	-8.5	6
KCl (1.6)	2026	6.12	14	-1.9	7
KBr (1.1)	2063	6.02	4	-4	6
CsI (4.8)	2420	5.13	0	0	5

The diamond sample DS-5 had remained for seven weeks in the photocell maintained at a vacuum of 6×10^{-4} mm of Hg when the second set of data was taken. In this set of measurements slight changes were made in the distances between the slits. Saturation currents were observed

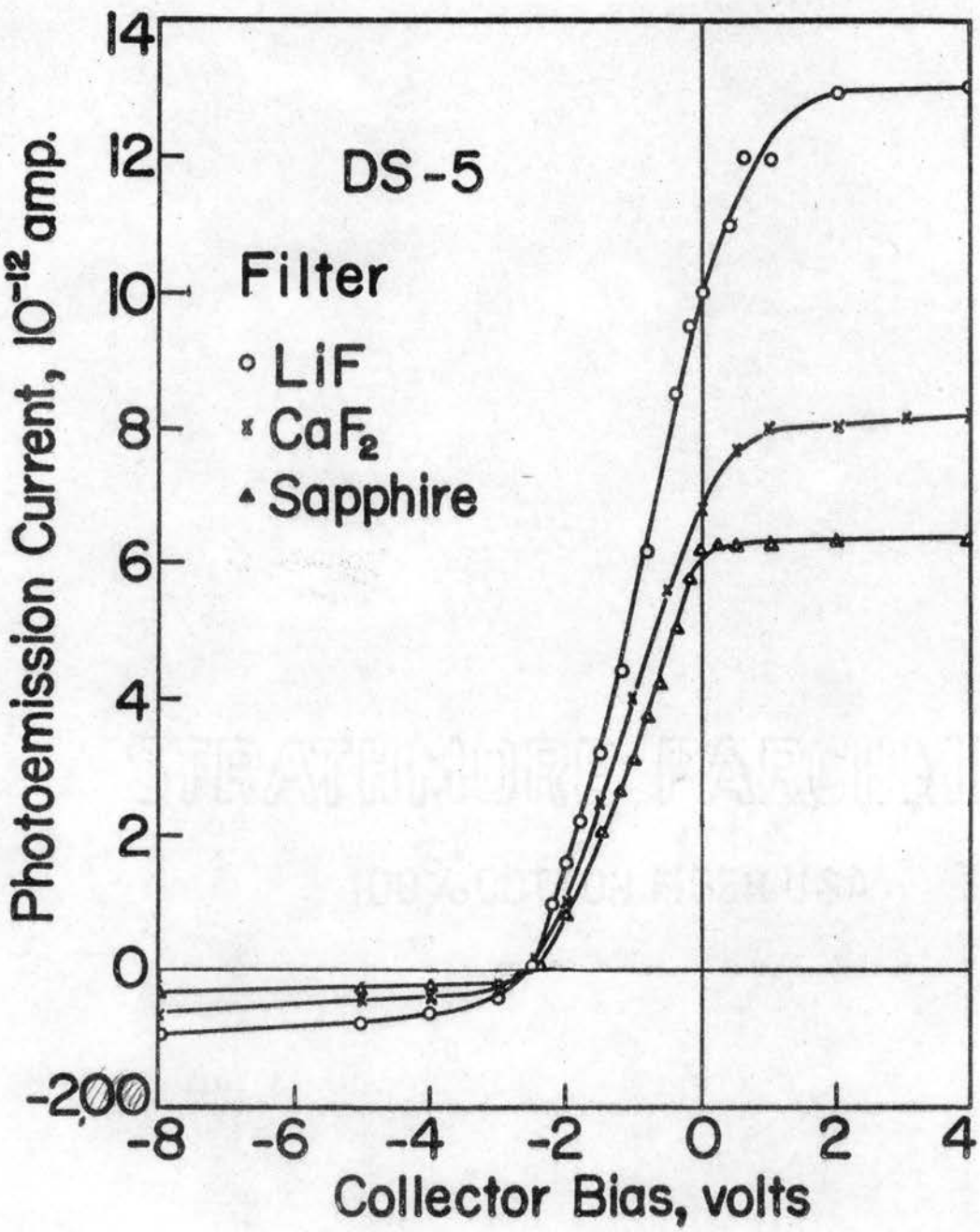

Fig. 19 (a). Photoemission current-potential characteristics for diamond DS-5

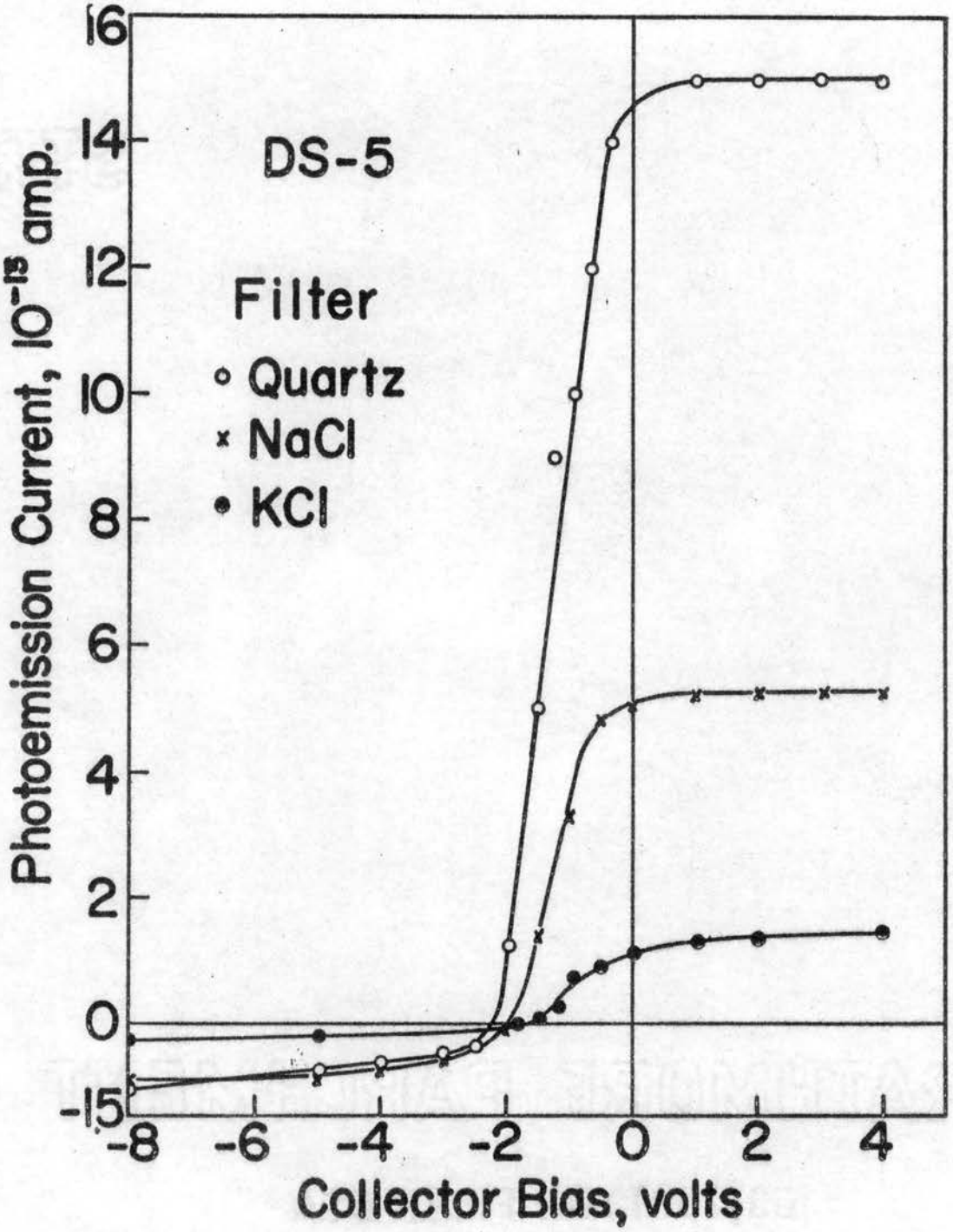

Fig. 19 (b). Photoemission current-potential characteristics for diamond DS-5

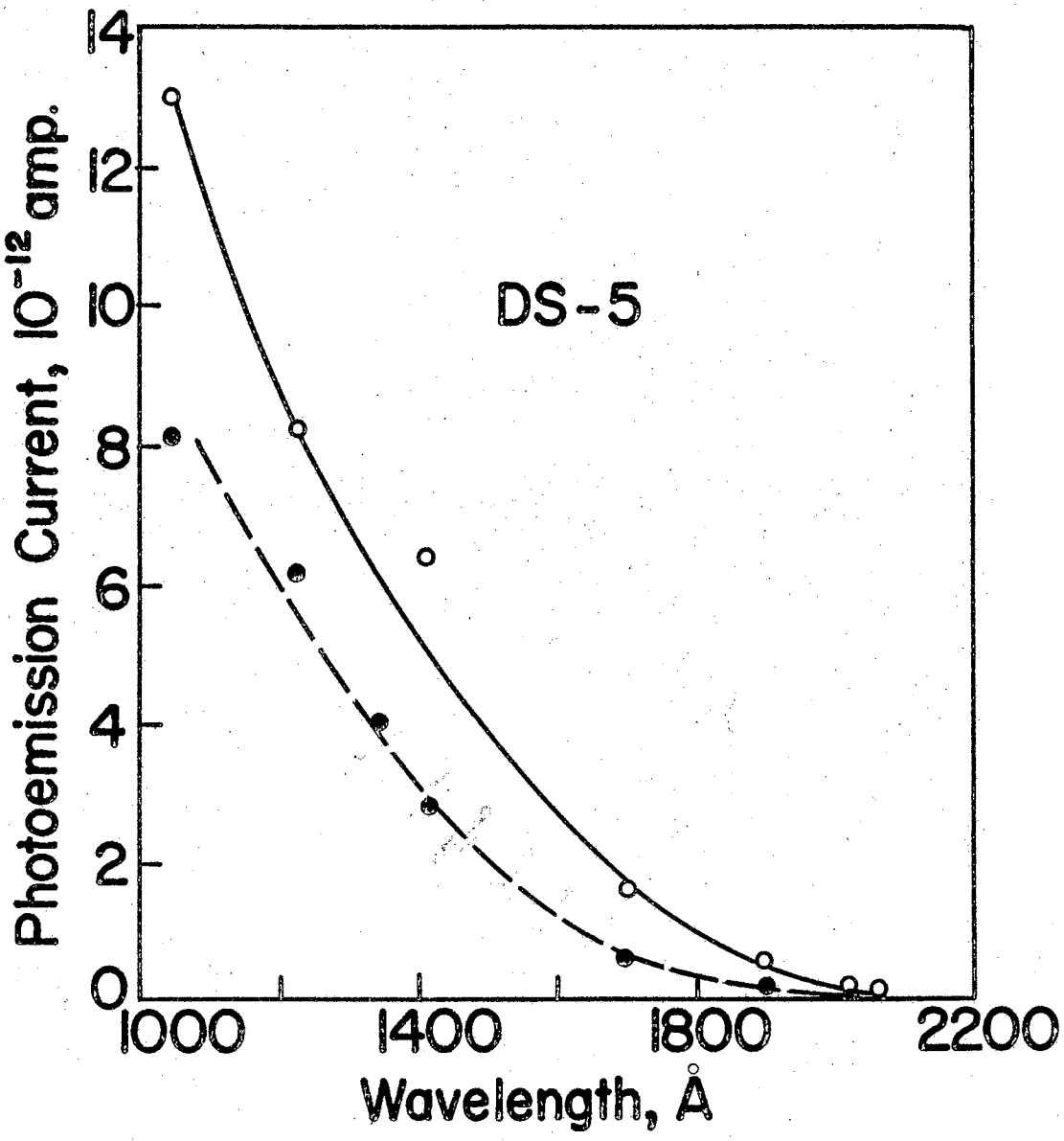

Fig. 20. Spectral distribution of the electron emission for diamond DS-5; o freshly cleaned sample, ● aged sample

when the collecting electrode was biased at either positive or negative five volts for each filter used. The results of the observations are given in Table VI while Fig. 20 shows the saturation currents plotted versus the short wavelength limit with a dashed line.

TABLE VI

SATURATION PHOTOEMISSION CURRENT FROM DIAMOND DS-5. (II)

Window or filter (mm)	Short wave length limit (Å)	Maximum photon energy (eV)	Saturation current (10^{-14} amp.)	Reverse current (10^{-14} amp.)
LiF (1.6)	1050	11.8	810	37
CaF_2 (1.7)	1230	10.0	620	28
BaF_2 (1.6)	1350	9.17	400	10
Sapphire (0.50)	1420	8.74	280	5.5
Quartz (4.0)	1700	7.30	55	4
NaCl (1.6)	1900	6.52	19	0.6
KCl (1.6)	2026	6.12	1.1	0
KBr (1.0)	2063	6.02	0	0

The curves in Fig. 20 show that the saturation photoemission currents obtained from the freshly cleaned sample surface are generally higher than those obtained from its aged sample surface and the curve for the aged sample cuts the abscissa axis at a shorter wavelength of light. The photoelectric threshold energy for the electron emission from diamond DS-5 falls in the range between 6.02 eV and 6.12 eV; the shift caused by the aging is about 0.1 eV. These are about the same results which were obtained for diamond DS-2.

When the square root of the photoemission current is plotted versus the exiting photon energy, the curve is almost a straight line as shown in Fig. 21. Small deviations could appear if more detailed investigations could be made. The straight line indicates that the photoemission

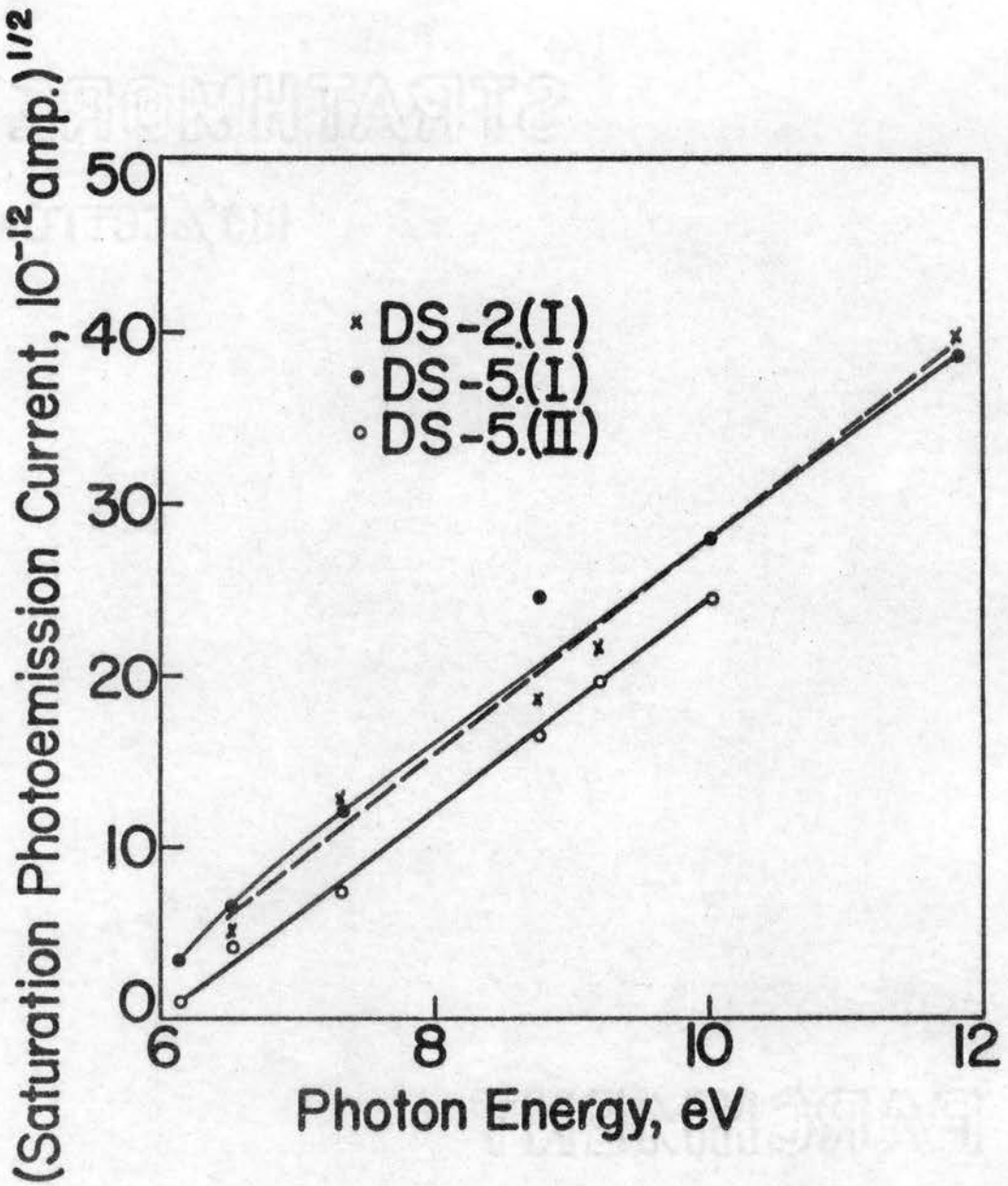

Fig. 21. Square root of photoemission current versus photon energy for diamonds

current is proportional to the square of the exciting photon energy which is not larger than 12 eV.

Photoelectric Emission From N-Type Germanium

Photoelectric emission from germanium sample Ge-1 was measured in the same manner as it was measured for the diamond DS-2. When the photoelectric emission current-potential characteristics were measured, the slit S_2 was 2 mm in diameter. In other measurements slit S_2 varied from 2 mm to 0.70 mm in diameter. The light source was a carbon arc operated in nitrogen gas at a pressure of 110 mm of Hg.

The photoelectric emission currents were observed on a freshly etched and cleaned sample surface by varying the collecting potential of the collecting electrode when the pressure of the photocell was maintained at 10^{-4} mm of Hg and when the incident light was filtered through the LiF windows. These measurements were repeated with a 4 mm thick quartz plate used as a filter for the light source. The current-potential characteristics from these measurements are shown in Fig. 22. The figure shows that the saturation current dropped drastically when the incident light was filtered by the quartz filter.

The germanium Ge-1 with sample holder was demounted from the photocell immediately after the above measurements and stored in a desiccator for a period of five months. The sample assembly was then removed from the desiccator, washed with distilled water, acetone and iso-propanol, and was mounted again into the photoelectric cell. The photocell was evacuated to a vacuum of 4×10^{-8} mm of Hg for further photoelectric

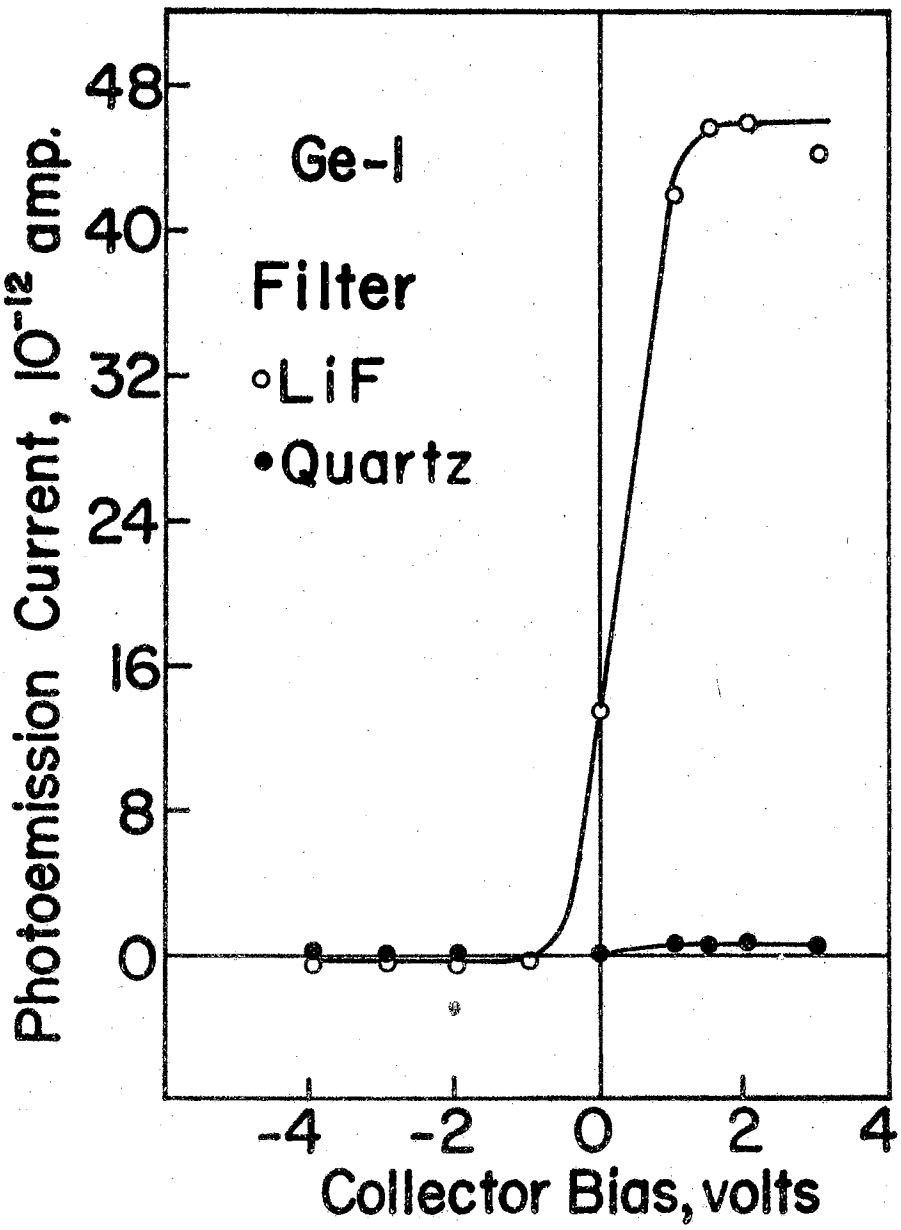

Fig. 22. Photoemission current-potential characteristics for Germanium Ge-1

emission measurements. Saturation currents were observed on this aged sample surface when various filters and different sizes of slits were used. The results are presented in Table VII. The collecting electrode was biased either positive or negative five volts.

TABLE VII

SATURATION PHOTOEMISSION CURRENT FROM GERMANIUM Ge-1

Window or filter (mm)	Diameter of slit S_2 (mm)	Saturation current (10^{-14} amp.)	Reverse current (10^{-14} amp.)
LiF (0.8)	0.70	680	---
Quartz (2.0)	0.70	35	---
Quartz (2.0)	1.32	245	---
KBr (1.0)	1.32	62	---
Corning glass 7910 (1.5)	2.0	26	16
CsI (2.2)	2.0	0	0
KI (4.8)	2.0	0	0

No photoelectric emission current was observed when the incident light was filtered through KI and CsI filters. The short wavelength limit of KI filter is 2540 Å and that of CsI is 2420 Å. The results indicate that the photoelectric threshold wavelength for the production of photoelectrons in this aged germanium sample Ge-1 is shorter than 2420 Å, corresponding to a photon energy 5.15 eV. On the other hand, the light, after passing through Corning Glass 7910 filter, did produce a feeble current. This filter has 10% transmission for light of wavelength 2250 Å which corresponds to a photon energy of 5.5 eV. Therefore, the photoelectric threshold for the production of photoelectrons from this aged germanium is between 5.15 eV and 5.5 eV, and the value 5.4 eV is justifiable.

CHAPTER V

DISCUSSION OF RESULTS AND CONCLUSION

Summary of Experimental Results

The results of these investigations of the photoelectric emission from natural semiconducting diamonds and from n-type germanium in the extreme ultraviolet light region are summarized below.

1. Photoelectric emission was observed from Type IIb diamonds with exciting light in the range of wavelengths from 1050 Å to 2060 Å.
2. The photoelectric threshold for the emission of electrons from Type IIb diamonds is approximately 6.02 eV as determined by plotting the diminishing saturation photoemission current against the increasing wavelength of the exciting light.
3. Photoelectric emission current from Type IIb diamonds was found to be lower when it was measured on a sample which had been mounted in an evacuated photocell for a few weeks (aged).
4. The photoelectric threshold energy for electron emission from Type IIb diamonds shifted to higher values when it was measured for an aged sample.
5. Photoelectric emission currents from a Type IIb diamond were higher when the pressure in the photocell containing the diamond was higher due to the adsorption of gases on the surface rather than photoionization of the gas.

6. The photoemission current from Type IIb diamonds is found generally to be proportional to the square of the exciting photon energy.
7. For the purpose of checking the apparatus and circuit connections, photoelectric emission currents from an n-type germanium sample were observed with incident light filtered through a LiF crystal and a quartz plate on the freshly etched and cleaned sample. The current-potential characteristics have the same form as those for Type IIb diamonds.
8. Saturation photoelectric emission currents from aged germanium were observed with incident light filtered through various filters. The photoelectric threshold for electron emission was found to be 5.4 eV, a value almost equal to those obtained previously by others (28, 52-55).
9. Photoelectrons were also emitted from the silver surface of the electrode being hit by the reflecting light from the diamond or germanium. This effect is indicated by the presence of the negative currents in the plots of the current-potential characteristics.

Photoelectric Emission from Germanium

The photoelectric emission from germanium was studied for two major reasons: To check the measuring equipment which was also used for the measurements on the diamond and to observe the general phenomena of photoemission currents which should be comparable to that of diamond. The photoemission current-potential characteristics obtained for the germanium are indeed similar to those obtained for the diamond. This is

clear when we compare the results for diamond DS-2 plotted in Fig. 15 and that for germanium Ge-1 plotted in Fig. 22. These two sets of data were taken under almost identical conditions, and both samples were freshly cleaned when the data were taken. With the incident light was filtered through a quartz filter and a LiF window, the saturation photoemission currents were found to be higher for diamond than those for germanium. With the incident light filtered through a LiF window alone, the saturation photoemission currents were also found to be higher for diamond than those for germanium. Such a comparison may prove the correctness of Van der Ziel's (16) calculation on the probability of the escape of the photoelectrons in which he showed more favorable photoemission in a semiconductor of larger energy gap.

Photoelectric emission from germanium has been studied by several people. Apker, Taft and Dickey (28) obtained 4.8 eV for the work function of p-type evaporated film. The Fermi level was between 0.10 eV and 0.18 eV from the top of the valence band. Haneman (52) obtained a value of 4.75 eV on a surface of a p-type crystal broken in high vacuum and showed the Fermi level to be 0.2 eV above the valence band edge. Suhrmann, Kruel and Wedler (53) obtained the photoelectric threshold for the electron emission from p-type germanium film as varying from 4.98 eV to 5.08 eV and showed the photoelectrons as originating at the surface states near the valence band edge.

Gobeli and Allen (54) made high vacuum studies of photoelectric emission and work function of cleaved germanium (111) faces. Their data show that the threshold emission was from filled surface states above the valence band edge and that the Fermi level was locked at the surface by the surface states. They obtained the photoelectric threshold as

4.80 ± 0.02 eV and the work function as 4.80 ± 0.04 eV. The fact that this value of the photoelectric threshold is equal, within their experimental uncertainty, to the work function means appreciable emission from filled levels immediately beneath the Fermi level.

Dillon and Farnsworth (55) measured the photoelectric threshold for the electron emission and the work function of germanium with a wide range of doping concentrations. For an intrinsic sample (48 ohm-cm), the photoemission threshold and the work function were 4.68 eV and 4.78 eV respectively, and for a highly doped sample (0.08 ohm-cm), they were 4.68 eV and 4.73 eV respectively. The Fermi level was 0.1 eV or less lower than the photoelectric threshold level in both cases, since the doping raised the Fermi level but also raised the surface barrier. We see that the net changes in the threshold energy for the electron emission and the work function because of doping were very small. By exposing the sample to oxygen, Dillon and Farnwsorth obtained about 5.0 eV for both the photoelectric threshold for electron emission and the work function; however, the Fermi level was raised above the threshold level by approximately 0.05 eV. Therefore, we see that the Fermi level was less than ±0.1 eV from the photoemission threshold level for samples in a wide range of doping and for samples with a clean as well as an oxidized surface.

In our measurements on the aged n-type germanium sample Ge-1, the photoelectric threshold for the electron emission was found to be 5.4 eV. Assuming the correctness of the findings of Gobeli and Allen that the photoelectric threshold for electron emission is equal to the work function and of Dillon and Farnsworth (55) that the energy separation between the Fermi level and the photoemission threshold level in

germanium is less than 0.1 eV, the work function of the germanium sample Ge-1 should be about 5.4 eV. This value is rather large, since the measurements were taken on a sample five months after etching, and the adsorption of oxygen on the surface could increase the work function as much as 0.3 eV. We had no intention to determine this value accurately, because the reasons for the measurements on germanium were to check the apparatus for spurious emission and to compare the emission phenomenon in general.

The Photoelectric Threshold of Diamond

According to the theoretical model of the photoelectric emission for semiconductors proposed by Gobeli and Allen (31), the photoelectric threshold is the indirect transition of the electrons from the top of the valence band at $\bar{k}$ (000) to the conduction band at $\bar{k}_{\varphi}$ where the conduction band intercepts the vacuum level as shown in Fig. 5. In an intrisic semiconductor which has constant bands from the bulk to the surface, the photoelectric threshold for electron emission is $h\upsilon_i(o)$. In a semiconductor which has band bending, it is expressed as $h\upsilon_i(x)$. The value of $h\upsilon_i(x)$ is smaller than that of $h\upsilon_i(o)$ if the band bending is downward from the bulk to the surface and is larger if the band bending is upward from the bulk to the surface.

This simple model concerning the transitions of the photoelectrons between two bands in semiconductors is useful in explaining experimental data for silicon; it is also in agreement with Kane's (30) theoretical systematic treatment of the photoelectric emission for all possible processes.

The crystal structure of silicon and diamond is the same, and their band structure is also similar. Both silicon and diamond have the tops of the valence bands at $\bar{k}$ (000), and at least on conduction band has

its maximum along the <111> direction (2, 31). Therefore, the simple model concerning the transitions of the photoelectrons in the photoelectric emission could be applied to diamond.

In accordance with previous measurements of rectification on diamond DS-2, the energy bands are bending downward from the bulk to the surface because of occupied surface states which may be produced by adsorbed ions, crystal imperfections or impurities near the crystal surface (36). Since both diamonds DS-2 and DS-5 are of p-type conductivity, the potential barrier at the surface should have conditions as shown in Fig. 5(b). Therefore, the value of $h\nu_i(x)$ is smaller than that of $h\nu_i(o)$, and the first emitting electrons excited by the photons with threshold energy are the electrons originating at a distance x beneath the surface.

According to Bardeen (56), the work function of a solid is determined by the emission of electrons from the top few layers of atoms. Therefore, the value of x, the escape length, must be of the order of 10^{-8} cm. This value is much smaller than the thickness of the surface barrier layer of a semiconductor which is of the order 10^{-6} to 10^{-4} cm. Therefore, a photoelectron which originates at a distance x beneath the surface and makes an indirect transition between the valence band and the conduction band to the vacuum after absorbing a photon of energy $h\nu_i(x)$ is the surface photoelectric effect.

If the energy band bending is gradual near the surface, the value of $h\nu_i(x)$ may be very little different compared to the value of $h\nu_i(o)$. Any means that could straighten the energy bands would increase the photoelectric threshold energy for the electron emission. This is the situation in diamonds DS-2 and DS-5 where the oxygen adsorbed surfaces of

aged samples straightened the energy bands, and the samples had a higher photoelectric threshold energy for the electron emission. Such a result can be explained more clearly with the help of Fig. 5(b). When it represents the condition of a freshly cleaned surface of a diamond sample, the positive charges on the surface may be due to water vapor or ionized impurity atoms. When the surface becomes aged, it is covered with a layer of adsorbed gas which contains negative charges. The negative charges neutralize the original positive charges, and the result is straightening of the energy bands. This means the energy bands in the bulk of the crystal are pulled down from the vacuum level, and the photoelectric threshold for electron emission, $h\nu_i(x)$, becomes larger. The effect of surface aging on the photoelectric threshold for electron emission from diamonds was found to be about 0.1 eV in our measurements, that from germanium amounting to 0.3 eV obtained by Dillon and Farnsworth (55); therefore, diamonds can be kept cleaner and the surface barrier is less sensitive to environmental changes.

The straightness of the energy bands and the shift of the photoelectric threshold for electron emission could be partly due to the exposure of the sample to the ultraviolet light which produced defects and knocked ionized impurity atoms from the surface. Illumination of germanium with a microscope lamp has been observed by Dillon and Farnsworth (55) to increase the work function by 0.09 eV.

As mentioned earlier, Spicer (21), in investigating the photoelectric emission from alkali antimonides at two different temperatures, confirmed the fact that the photoelectrons emitted from a p-type semiconductor originate at acceptor energy levels in the low yield area. Accordingly, the small measurable photoemission currents which we

obtained for diamonds DS-2 and DS-5 were attributed to the electrons at the acceptor levels where they were excited by the photons with a threshold energy. The photoelectric threshold for emission from these diamonds was found to be 6.06 eV. Therefore, the vacuum level is 6.41 eV above the top of the valence band, and the electron affinity is about 0.9 eV. Such a band structure is similar to that of CsI which has optical absorption occurring at about 5.6 eV between two bands and an estimated electron affinity 0.3 eV (58).

The Work Function of Diamond

Natural Type IIb diamonds thus far are known to have p-type conductivity. Optical absorption data taken in this laboratory (33, 34, 38) and the temperature dependence of the resistivity of semiconducting diamond DS-1 measured by Leivo and Smoluchowski (57) show that the acceptor levels are about 0.35 eV above the valence band. A calculation of surface states on the (111) face of the diamond has been made by Pugh (18) based on the linear combination of band orbitals (LCBO) method. His results show a band of surface states lying somewhat below the middle of the energy gap. The width of the band of states is of the order of half the energy gap, but only a narrow band of high density of states is significant. Since half the surface states are filled, the Fermi level in the case of no band bending lies within this narrow band somewhat below the energy for which the density of states is a maximum. Therefore, the narrow band in which the states are filled in Pugh's calculation may be the impurity band of the acceptor levels. Dillon and Farnsworth (55) showed that the value of the work function and that of the photoelectric threshold for electron emission in germanium differ

very little. Gobeli and Allen's data (54), also in germanium, show that the photoelectric threshold for electron emission is, within the experimental uncertainty, equal to the work function. Scheer and Van Laar (22) found the photoelectric threshold for electron emission from the filled surface levels of p-type silicon and other materials is the work function, as measured by the contact potential method. They accordingly stated that such a surface would have a metallic characteristic and the threshold energy for surface state emission would always be equal to the work function obtained from contact potential measurements.

In regard to the results in germanium and silicon just stated and in diamond calculated by Pugh (18), we believe that the Fermi level in a natural semiconducting diamond lies within a narrow band of surface states. Since the effective width of the narrow band is small, the Fermi level must lie in the neighborhood of the filled surface states for which the density is maximum. The photoelectric threshold for electron emission of diamonds DS-2 and DS-5 was found to be 6.02 eV, therefore, the work function of the semiconducting diamonds is equal to 6.02 ± 0.1 eV.

According to equation (2.20), the Fermi level should lie below the acceptor level as long as N_a is 6 times larger than N_d. Otherwise, the Fermi level will be above the acceptor level. Since the natural diamond has p-type conductivity, it is likely that N_a is one order or more larger than N_d, and the Fermi level will lie below the acceptor level. Calculations from equation (2.20) show the Fermi level lying less than 0.10 eV below the acceptor level for a p-type diamond having a room temperature resistivity larger than 3 ohm-cm. Such a calculation also results in a small energy separation between the Fermi level and the acceptor level.

Experimental results from Hall coefficient measurements for diamond DS-2 indicate that $N_a = 3.25 \times 10^{16}$ cm^3, and $N_d = 9.5 \times 10^{15}$ cm^3 (32). By using these values in equation (2.20) and (2.23), the value of p is found to be approximately 5×10^{12} cm^3 and that of $(E_F - E_a)$ to be approximately 0.01 eV. This is again a negligible quantity.

The photovoltaic effects for contact between diamonds DS-2 as well as DS-5 and metals such as aluminum, silver, gold and platinum were investigated in this laboratory. The photovoltage for the contact between the semiconducting diamond and platinum was observed to be much smaller compared with that between the semiconducting diamond and other metals. This indicates that the heights of the potential barriers of diamonds DS-2 and DS-5 are close to that of platinum. The work function of platinum is 6.30 eV (59), and therefore there is a general agreement in our measurements

Photoemission Current in Diamond

When the energy of the photons is higher than the threshold for electron emission, photoelectrons will be emitted from the interior of the crystal at various depths. They will be emitted from both the acceptor levels and the valence band. The magnitude of the photoemission current depends upon the intensity of the exciting light of a given wavelength for a fixed illuminated area. In the ultraviolet light region of a carbon arc the intensity of the continuous spectrum first decreases rapidly with decreasing wavelength, it then decreases slowly between 2600 Å and 1700 Å. Below 2000 Å atomic line spectra mainly contribute to radiation. Atomic lines of the carbon arc are most intense in the region between 1150 Å and 1720 Å in the Schumann region. When the arc

is discharged in nitrogen, atomic spectra of nitrogen should also contribute to the radiation. Atomic lines of nitrogen in the region between 1060 Å and 1200 Å have a very high intensity. There is also a band of lines between 1720 Å and 1950 Å having a lower intensity. All these atomic lines of carbon and nitrogen atoms contributed to the photoemission currents in our measurements.

Although the light source was not monochromatic, the short wavelengths of the spectrum were most effective in the production of the photoemission. The exponential decrease of the saturation current with the wavelength (short wave limit of filter) of the photons as shown in Figs. 17, 18, and 20 may be associated with the attenuation of light within the diamond to a certain degree, for the coefficient of absorption of light in diamond decreases with the wavelength in this region (60), and the intensity of the light within the crystal decreases exponentially in accordance with the absorption factor. However, the light source was not monochromatic and the intensity of the lines produced in the arc was not the same, it is difficult to say something very definitively.

When the square root of the saturation photoemission current is plotted versus the photon energy as shown in Fig. 21, the shape of the curves is almost a straight line. It appears as if the photoemission current is proportional to the square of the exciting photon energy. According to Kane's evaluation, such a relation would correspond to the production of the photoelectron from the surface states as well as from the volume and the electrons would make direct transitions. Again, the exciting light at various wavelengths has a different intensity and it is not monochromatic, therefore, this has to be taken into consideration.

As reviewed earlier, Tamm and Schubin (24), and Taft and Apker (25)

found no volume photoemission effect when the photon energy was less than twice the threshold energy. In the photoemission from diamonds the maximum energy of the exciting photons was less than twice the threshold energy for electron emission, but it is not clear whether there was a volume effect. There is confusion about the term volume effect. Electron emission from the interior of the crystal in the surface barrier layer is a volume effect from the viewpoint of geometry but is a surface effect from the viewpoint of energy.

The magnitude of the saturation photoemission currents obtained by using various filters could have been affected by the operating condition of the carbon arc and the condition of the sample surface. The burning away of the carbon weakened the intensity of the light source; the bombardment of the ultraviolet light on the sample produced defects and removed the ionized impurity atoms; and the generally aged sample surface possibly covered with a layer of oxygen atoms, reduced the sensitivity of response to light. This is why the photoemission current was generally higher when it was first observed from a freshly cleaned sample.

The negative currents as shown in the plot of photoemission current-potential characteristics were mostly contributed to the photoemission of electrons from the inner silver surface in which the surface acted as the collecting electrode. Silver has a photoelectric work function of 4.7 eV. Data obtained by Philipp and Taft (60) show the reflectance of the diamond being 22% or more in the wavelength range of light from 2000 Å to 1050 Å, and therefore the scattering of light from the diamond surface would definitely hit the silver surface which would emit electrons. The photoemission from surfaces other than the diamond effects

the accuracy of the threshold of emission of the sample being determined, but those spurious emission have been carefully minimized.

There are, of course, many ways in which the present work could be improved given sufficient time. Now that the general method of using the photoelectric emission technique is believed to be reliable, desirable refinements would include repeating the measurements with a vacuum ultraviolet monochromator instead of the filters which were used here. A vacuum ultraviolet monochromator was not available for this work. Also, although difficult to obtain accurately for the vacuum ultraviolet range involved, it would be most desirable to obtain a reasonably accurate distribution of the intensity of the light from the carbon arc instead of using information obtained indirectly from arcs operated under similar conditions.

BIBLIOGRAPHY

1. W. Shockley, Electrons and Holes in Semiconductors, (D. Van Nostrand Co., Inc., New York, 1950).

2. F. Herman, Phys. Rev. 88, 1201 (1952); Ph.D. Dissertation, (Columbia University, 1953).

3. C. D. Clark, P. J. Dean and P. V. Harris, Proc. Roy. Soc. (London) 277, 312 (1964).

4. R. Robertson, J. J. Fox and A. E. Martin, Phil. Trans. Roy. Soc. London 232, 463 (1934).

5. J. F. H. Custer, Physica 18, 1489 (1952).

6. J. F. H. Custer, Physica 20, 183 (1954).

7. P. Tartakowsky, Z. Physik 58, 394 (1929).

8. B. Edlen, Report on Progress Physics 5, 210 (1939).

9. A. G. Shenstone, Report on Progress Physics 26, 181 (1963).

10. R. Tousey, Appl. Opt. 1, 679 (1962).

11. F. Seitz, Modern Theory of Solids, (McGraw-Hill Book Co., Inc., New York, 1940).

12. E. Wigner, Phys. Rev. 46, 1002 (1934).

13. R. H. Fowler and E. A. Guggenhein, Statistical Thermodynamics, (Cambridge University Press, London, 1949).

14. C. Kittel, Introduction to Solid State Physics, (John Wiley and Son, Inc., New York, 1957), 2nd ed.

15. J. S. Blakemore, Semiconductor Statistics, (Pergamon Press Inc., New York, 1962).

16. A. Van der Ziel, Solid State Physical Electronics, (Prentice-Hall, Inc., New York, 1957).

17. W. Shockley, Phys. Rev. 56, 317 (1939).

18. D. Pugh, Phys. Rev. Letter 12, 390 (1964).

19. J. Bardeen and S. R. Morrison, Physica 20, 873 (1954).

20. I. Tamm, Phys. Z. Sojet 1, 733 (1932).

21. W. E. Spicer, Phys. Rev. 125, 1297 (1962); Phys. Rev. 112, 114 (1958); J. Appl. Phys. 31, 2077 (1960).

22. J. J. Scheer and J. Van Laar, Physics Letters 3, 246 (1963).

23. L. Apker and E. Taft, Phys. Rev. 79, 964 (1950); Phys. Rev. 81, 698 (1951).

24. I. Tamm and S. Schubin, Z. Physik 68, 97 (1931).

25. E. Taft and L. Apker, J. Opt. Soc. Am. 43, 81 (1953).

26. R. H. Fowler, Statistical Mechanics, (Cambridge University Press, London, 1936).

27. H. B. Huntington and E. Taft, Phys. Rev. 89, 352 (1953).

28. L. Apker E. Taft and J. Dickey, Phys. Rev. 74, 1462 (1958); Phys. Rev. 76, 270 (1949).

29. D. Redfield, Phys. Rev. 124, 1809 (1961).

30. E. O. Kane, Phys. Rev. 127, 131 (1962).

31. G. W. Gobeli and F. G. Allen, Phys. Rev. 127, 141 and 150 (1962).

32. W. J. Leivo, et al., Investigations of Semiconducting Properties of Type IIb Diamonds, Report No. AFOSR-2642, Office of Aerospace Research, U. S. Air Force, Washington 25, D. C.

33. H. J. Stein, M. D. Bell and W. J. Leivo, Bull. Am. Phys. Soc. 1, 127 (1956); C. C. Johnson and W. J. Leivo, Bull. Am. Phys. Soc. 3, 114 (1958).

34. H. J. Stein, M. D. Bell and W. J. Leivo, Color Center Symposium, Argonne National Laboratory, (Nov., 1956).

35. M. D. Bell and W. J. Leivo, Bull. Am. Phys. Soc. 1, 382 (1956).

36. M. D. Bell and W. J. Leivo, Bull. Am. Phys. Soc. 2, 171 (1957); Phys. Rev. 111, 1227 (1958).

37. J. H. Wayland and W. J. Leivo, Bull. Am. Phys. Soc. 3, 400 (1958).

38. C. Johnson, et al., J. Phys. Chem. Solids 25, 827 (1964).

39. J. B. Krumme and W. J. Leivo, Bull. Am. Phys. Soc. 5, 189 (1960).

40. M. D. Bell and W. J. Leivo, Bull. Am. Phys. Soc. 6, 142 (1961).

41. R. Gore, Perkin-Elmer Instrument News 13, 6 (1962).

42. S. S. Ballar, L. S. Combes and K. A. McCarthy, J. Opt. Soc. Am. 42, 684 (1952).

43. L. Kunkelman, W. B. Fowler and J. Hennes, Appl. Opt. 1, 698 (1962).

44. R. W. Kebler, Properties of Synthetic Sapphire, (Linde Company, New York).

45. R. A. Sawyer, Experimental Spectroscopy, (Prentice-Hall, Inc., New York, 1944).

46. H. C. Kremers, Inc. and Eng. Chem. 32, 1478 (1940).

47. G. R. Harrison, R. C. Lord and J. R. Loofborrow, Practical Spectroscopy, (Prentice-Hall, Inc., New York, 1948).

48. Z. Gyulai, Z. Physik 46, 80 (1927).

49. W. R. Brode, J. Phys. Chem. 30, 56 (1926).

50. S. S. Ballard, L. S. Combes and K. A. McCarty, J. Opt. Soc. Am. 43, 975 (1953).

51. P. Palesky, R. K. Swark and R. Grenchik, Rev. Sci. Inst. 18, 299 (1947).

52. D. J. Haneman, J. Phys. Chem. Solids 11, 205 (1959).

53. R. Suhrmann, M. Kruel and G. Wedler, Z. Physik 173, 71 (1963).

54. G. W. Gobeli and F. G. Allen, Surface Science 2, 402 (1964).

55. J. A. Dillon and H. E. Farnsworth, J. Appl. Phys. 28, 174 (1957).

56. J. Bardeen, Phys. Rev. 49, 653 (1936).

57. W. J. Leivo and R. Smoluchowski, Phys. Rev. 98, 1532 (1955).

58. H. R. Philipp and E. A. Taft, J. Phys. Chem. Solids 1, 159 (1956).

59. L. A. DuBridge, Phys. Rev. 31, 236 (1928).

60. H. R. Philipp and E. A. Taft, Phys. Rev. 127, 159 (1962).

VITA

Whua Fu Wei

Candidate for the Degree of

Doctor of Philosophy

Thesis: PHOTOELECTRIC EMISSION AND WORK FUNCTION OF SEMICONDUCTING DIAMONDS

Major Field: Physics

Biographical:

Personal Data: Born in Laipor, China, October 27, 1920, the son of Show Kow and Sue Ching Wei.

Education: Attended graduate school in Marlin and Kweilin, China; graduated from Kweilin High School; received Bachelor of Science degree from National Chekiang University in Hangchow, China, with a major in physics, in June, 1943; attended Indiana University and University of Colorado; received the Master of Science degree from the Oklahoma State University with a major in physics, in May, 1951; completed requirements for the Doctor of Philosophy degree in May, 1965.

Experience: Taught in University in China for more than five years; worked in Delco Radio Division of General Motors Corporation and the University of Colorado for over five years.

Organizations: Member of Sigma Pi Sigma, Pi Mu Epsilon, and associate member of Sigma Xi.